



## A comparative investigation for identification of N-(4-dimethylamino 3,5-dinitrophenyl)maleimide

Seda Karaboğa<sup>1</sup> , Gürcan Yıldırım<sup>2</sup> 

### Keywords:

*N-(4-dimethylamino 3,5-dinitrophenyl)maleimide, DFT-HF calculations, HOMO and LUMO, MEP, Molecular structure*

**Abstract** — This study has identified the characteristic behaviors of N-(4-dimethylamino 3,5-dinitrophenyl)maleimide molecule using ab initio Hartree-Fock (HF) and density functional theory (DFT) based on Becke's three-parameter hybrid exchange functional combined with Lee-Yang-Parr non-local correlation function (HF/B3LYP and DFT/B3LYP) at 6-311G++(d,p) level of theory for the first time. On this basis, the optimized molecular structures, some thermodynamic features at 300 K, function groups of structures, charge distributions-dipole moments, molecular charge transfer regions, spectroscopic characteristic properties, vibrational frequencies, nuclear magnetic resonance chemical shifts of <sup>13</sup>C-NMR and <sup>1</sup>H-NMR spectra, and corresponding vibrational assignments have been investigated in detail. Comparisons between some experimental findings and theoretical results are performed to test the reliability of the calculation method preferred in the study. The comparison results in high correlation parameters such as R<sup>2</sup> =0.976 and R<sup>2</sup> =0.985 for the molecular structures and vibrational frequencies in the DFT and HF calculation levels, respectively. Moreover, the obtained vibrational frequencies and calculated results are in good agreement with the experimental data. Additionally, the simulations of highest/lowest occupied/unoccupied molecular orbital (HOMO and LUMO), molecular electrostatic potential (MEP), and electrostatic potential (ESP) maps have shown that there appear strong non-uniform intramolecular charge distributions (ICT), electron engagements, lone pairs of electrons, π-π\* conjugative effects based on the bond weakening, and intermolecular hydrogen bonding in the compound. Correspondingly, the molecule with the electrophilic reactive and nucleophilic regions has been noted to exhibit kinetical chemical stability. All the discussions have been confirmed by means of the findings of optimized molecular structures and vibrational frequencies belonging to the molecule.

**Subject Classification (2020):**

## 1. Introduction

Heterocyclic compounds have widely been utilized in the pharmaceutical industry due to their alluring properties, including the physicochemical, selective affinity towards biomolecules, and constructive as therapeutics agents. Maleimides are one of the most promising classes of heterocyclic compounds having the formula of H<sub>2</sub>C<sub>2</sub>(CO)<sub>2</sub>NH. The compound together with other organics have extensively been used in biological applications as anti-protozoal [1], anti-angiogenic [2], anti-bacterial [3], and anti-

<sup>1</sup>tanyildizi\_s@ibu.edu.tr (Corresponding Author); <sup>2</sup>yildirim\_g@ibu.edu.tr

<sup>1</sup>Department of Chemistry, Faculty of Arts and Sciences, Bolu Abant İzzet Baysal University, Bolu, Türkiye

<sup>2</sup>Department of Mechanical Engineering, Faculty of Engineering, Bolu Abant İzzet Baysal University, Bolu, Türkiye

Article History: Received: 23 Jan 2023 — Accepted: 12 Apr 2023 — Published: 30 Apr 2023

stress agents [4]. Especially, N-substituted ones are an essential part of electron acceptors that can form charge transfer complexes with several vinyl monomers [5,6].

In recent years, it has been reported that derivatives of maleimides could be used as selective inhibitors for monoglyceride lipase [7], Bfl-1 [8], and DNMT-1 protein [9]. Several researchers have investigated the biological activity of N-substituted derivatives of maleimides in the last ten years and obtained successful medical results on this issue. Zacchino and coworkers have reported that the N-substituted maleimides have shown anti-microbial activity against *Candida* spp [10]. They also observed that the maleimide framework had played a staminal role in the increase in the biological activity of these compounds. The structure-dependent antifungal activity of N-substituted maleimides was reported by Salewska et al. in 2012 [11]. Therefore, a great interest has begun in the synthesis of maleimides derivatives. In addition to the interest in the biological area, the N-substituted maleimides, with their excellent heat resistance, have also been used to prepare various polymers and copolymers. In other hands, the characteristic heat resistance property enables the N-substituted maleimides to be utilized in several areas, such as in rubber, plastics, and proteins [12,13]. Hence, the N-substituted maleimides are essential in organic chemistry, the polymer industry, and biological science.

Moreover, many studies on the N-substituted maleimides have been performed, and the scientific works have increased on the theoretical and experimental investigations of N-(4-dimethylamino 3,5-dinitrophenyl)maleimide, and its derivative organic compounds day by day. Reliable and effective results of theoretical investigations are much more important for the characteristic features of molecules as structural, thermodynamical, charge distributions-dipole moments, molecular charge transfer regions, and optical, spectroscopic, and electrochemical characteristic properties [14]. In other hands, a suitable quantum chemical method allows us to economically predict the compound characteristics and elucidate some experimental phenomena insightfully [15].

In the modern theoretical world, density functional theory (DFT) and ab initio Hartree Fock (HF) obtained considerable popularity as an effective general procedure to examine the physical, structural, thermodynamical, charge distributions dipole moments, molecular charge transfer regions, spectroscopic, and optical properties of the new synthesized molecules. In the current work, the molecular structures (optimized structures, bond lengths, bond angles, and bond dihedrals) and vibrational frequencies were calculated using ab initio Hartree-Fock (HF) and density functional theory (DFT) based on Becke's three-parameter hybrid exchange functional combined with Lee-Yang-Parr non-local correlation function (HF/B3LYP and DFT/B3LYP) at 6-311G++(d,p) level of theory. All the theoretical findings were compared to the experimental results obtained SDBS (13095) database [16]. It was found that the comparisons between experimental and theoretical findings have been noted to present a good correlation. This shows the reliability of the theoretical approach models used in the present three studies. Moreover, the vibrational frequencies, infrared intensities, and vibrational assignments were inspected.

Furthermore, the values of the energy band gap and transition states were examined concerning the frontier orbitals (the energy difference between HOMO and LUMO results). The maps relating to the molecular electrostatic potential (MEP), electrostatic potential (ESP),  $^{13}\text{C}$ , and  $^1\text{H}$  chemical shifts of the compounds have been researched to find both the electrophilic/nucleophilic regions and the chemical stability (founded on the strong non-uniform intra-molecular charge distributions (ICT), electron engagements, lone pairs of electrons,  $\pi$ - $\pi^*$  conjugative effects, and intermolecular hydrogen bonding) of the compound studied. This study is interested in not only giving information about the identification of N-(4-dimethylamino 3,5-dinitrophenyl)maleimide and presenting in detail the vibrational modes but exhibit the way to future research, functionality in the medical areas (cytotoxic, anti-malarial, pharmacological activities), applications in biology and industry areas of this molecule.

## 2. Computational Details

The optimized molecular structures, thermodynamic features at 300 K, functional groups of structures, charge distributions-dipole moments, molecular charge transfers, spectroscopic properties, vibrational frequencies, corresponding vibrational assignments, and NMR chemical shifts of N-(4-dimethylamino 3,5-dinitrophenyl)maleimide molecule have been studied via Gaussian 09 package program [17,18] at HF and B3LYP/6-311++G(d,p) [19-22] level of theory for the first time. Besides, Electrochemical features such as highest/lowest occupied/unoccupied molecular orbitals (HOMOs and LUMOs), molecular electrostatic potential (MEP), and electrostatic potential (ESP) maps, energy band gap parameters, and transition states have been simulated.

## 3. Results and Discussion

According to Figure 1, the title compound possesses 32 atoms for a molecule and belongs to point group C<sub>1</sub> including only the identity operation symmetry element; accordingly, all frequency modes (vibrations) are produced in only A species. As is well-known from the spectral analysis, the N atomic molecules provide 3N internal modes [23, 24] due to the existence of 3-dimensional space since every atom possesses 3 degrees of freedom. All the atoms are bonded and move translational, rotational, and vibrational. Thus, six modes (number of variables) appear for the translation and rotational modes for non-linear molecules. Three modes for the rotational movement stem from the rotations around three axes.

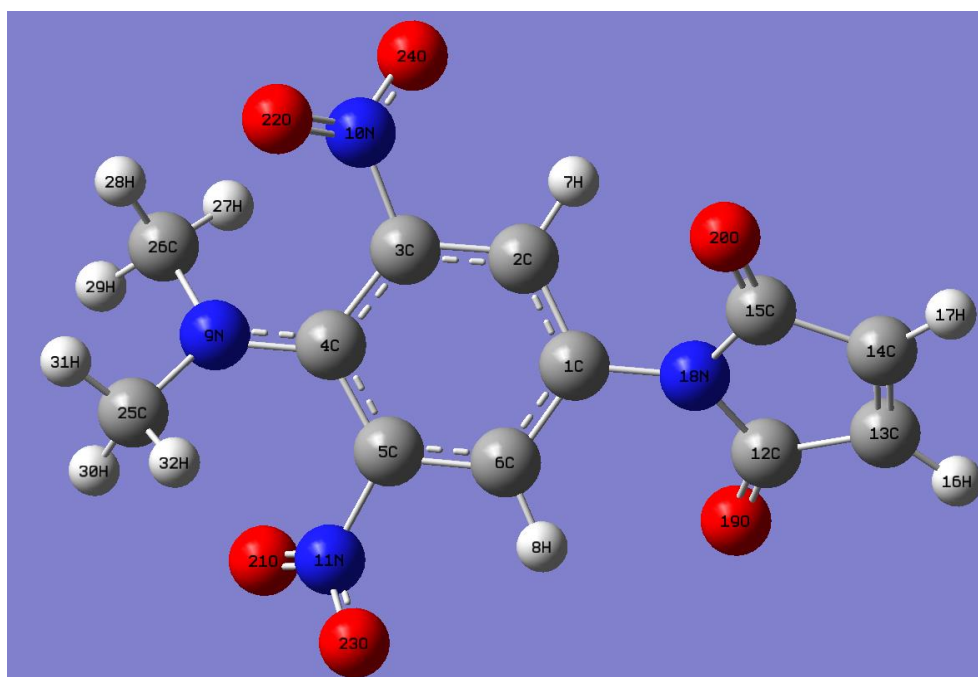


**Figure 1.** Optimized molecular structure of N-(4-dimethylamino 3,5-dinitrophenyl)maleimide

Correspondingly, 90 (3N-6) degrees of freedom constitute vibrational motion in the molecule. In this study, we have performed a frequency calculation analysis to obtain the spectroscopic signature of N-(4-dimethylamino 3,5-dinitrophenyl)maleimide. Vibrational frequencies have been calculated by using HF/6-311++G(d,p) and DFTB3LYP/6-311++G(d,p) methods. According to the literature, the vibrational frequencies are required to be scaled because they are mostly higher than the experimental ones. Hence, the vibrational frequencies computed at DFT-B3LYP/6-311++G(d,p) basis set were scaled by 0.958 for wavenumbers if the values are greater than 1700 cm<sup>-1</sup>; otherwise, the scaling factor of 0.983 was used [25-28].

Moreover, the vibrational frequencies scaled by the factors of 0.9051 for HF/6-311++G(d,p) were given in Table 2. Thus, Tables 1 and 2 present the scaled vibrational frequencies compared with experimental values, Red. Masses, force Constant, IR intensities, Raman activity, Depolar(P) and Depolar(U) of the molecule, respectively. The correlation coefficient ( $R^2$ ) between the experimental and theoretical vibrational frequencies computed at DFT-B3LYP/6-311++G(d,p) basis set is found to be about 0.9996 (as provided in Figure 2), whereas the value of  $R^2$  is observed to be about 0.9977 (see Figure3) for the HF/6-311++G(d,p) level of theory. It is found that the data obtained from the computational programs seem to be in good agreement with the experimental results. This shows that the theoretical method preferred is reliable for getting information about frequencies for the N-(4-dimethylamino 3,5-dinitrophenyl)maleimide molecule.

As for the corresponding vibrational assignments of molecule studied, the existence of aromatic rings in a structure can easily be determined owing to the relation of C-H and C-C-C ring vibrations. As received, the multiplicity of C-H stretching bands seen between  $3000\text{ cm}^{-1}$  and  $3150\text{ cm}^{-1}$  are called the aliphatic C-H stretch [29]. For example, in a scientific study, the vibrations of C-H stretching bands have been observed in the  $3120\text{--}3000\text{ cm}^{-1}$  [30]. The vibrations related to the C-H stretching bands for the benzoxazole have been observed at  $3085, 3074, 3065,$  and  $3045\text{ cm}^{-1}$  band [31].

In the present work, the vibrational values of aliphatic asymmetrical and symmetrical C-H stretching band for the molecule were calculated to be about  $3114, 3096, 3095,$  and  $3094\text{ cm}^{-1}$  at B3LYP/6-311++G(d,p) level of calculation and  $3086, 3070,$  and  $3066\text{ cm}^{-1}$  at HF/6-311++G(d,p) level of calculation, respectively. The bands have been experimentally observed in the range of  $3082\text{--}3107\text{ cm}^{-1}$ . In the C-H stretching bands in the methyl groups, the vibration parameters were calculated to be about  $2996, 2995, 2944, 2939, 2894,$  and  $2887\text{ cm}^{-1}$  at B3LYP/6-311++G(d,p) level of calculation and  $2956, 2954, 2916, 2914, 2868,$  and  $2862\text{ cm}^{-1}$  at HF/6-311++G(d,p) level of calculation, respectively. The C-H stretching bands in the methyl groups have experimentally been recorded as  $2924$  and  $2964\text{ cm}^{-1}$ . Even is well known that the frequencies belonging to the methyl group have been noticed to appear at  $2970\text{--}2950$  or  $2880\text{--}2860\text{ cm}^{-1}$  [29]. All the calculations (especially performed by DFT method with superior correlations) have been observed to agree with the experimental measurement results.

Additionally, the maximum Raman activities have been calculated to be about  $517.00$  and  $349.09$  for the aromatic stretching  $\nu_{\text{sym}}(\text{CH}_3)$  vibrations by applying the B3LYP/6-311++G(d,p) and HF/6-311++G(d,p) levels of theory, respectively. Moreover, we have calculated the stretching vibration bands (carbonyl group modes) between the carbon and oxygen atoms. On this basis, the aromatic  $\nu_{\text{sym}}(\text{C}=\text{O}_2)$  modes have been observed to be approximately  $1720$  and  $1706\text{ cm}^{-1}$  in the experimental spectrum. The modes have been calculated to be about  $1759$  and  $1706\text{ cm}^{-1}$  at B3LYP/6-311++G(d,p) level of theory, while the bands have appeared at about  $1862$  and  $1798\text{ cm}^{-1}$  at HF/6-311++G(d,p) basis set. According to the comparisons, the DFT calculation level exhibits superior performance to the HF level of theory. Similar results have been seen in the literature [32].

Moreover, the differentiation in the stretching  $\nu_{\text{sym}}(\text{C}=\text{O}_2)$  vibration bands has resulted from varied  $\pi\text{-}\pi^*$  conjugative effects and electron donating groups leading to the strong non-uniform intra-molecular charge distributions, actual position of the substituents, electron engagements, and lone pairs of electrons over the molecule. Among the IR intensities (in the unit of  $\text{km/mol}$ ), the strongest IR bands have been noted to be about  $626.4407\text{ km/mol}$  and  $1003.786\text{ km/mol}$  for the stretching  $\nu_{\text{sym}}(\text{C}=\text{O}_2)$  vibration bands at B3LYP/6-311++G(d,p) and HF/6-311++G(d,p) levels of theory, respectively. As for the C-C stretching modes and C-C-C ring vibration bands in the benzene ring, in the literature, the inner modes have appeared at approximately  $1315\pm 65$  and  $1000\text{ cm}^{-1}$  bands, while the latter modes have been recorded at the bands of  $1600, 1580, 1490$  and  $1440\text{ cm}^{-1}$  [30].

In this study, the ring modes have been observed between 982 and 1593  $\text{cm}^{-1}$  bands at B3LYP/6-311++G(d,p) level of theory while the bands have appeared at intervals 1006-1666  $\text{cm}^{-1}$  at HF/6-311++G(d,p) basis set. The modes have experimentally been observed in the 1687-968  $\text{cm}^{-1}$ . The main difference between the experimental findings and theoretical calculations stems from two main reasons: (I) the experimental results have been taken in the solid phase, and theoretical calculations have been performed in the gas phase. (II) in the theoretical calculations, the  $\pi$ - $\pi^*$  conjugative effects and electron donating groups leading to the strong non-uniform intra-molecular charge distributions, actual position of the substituents, electron engagements, and lone pairs of electrons over the molecule have been anticipated to be more homogenous than those in the experimental results [33]. In the literature, to illustrate the 3-(5-methyl thiazole-2-yl-diazenyl)-2-phenyl-1H-indole under C1 symmetry, the main C-C stretching bands have been calculated between 1071 and 1567  $\text{cm}^{-1}$ .

Besides, the C-C stretching modes and C-C-C ring vibration bands have been found in the ranges from 1600  $\text{cm}^{-1}$  to 1585  $\text{cm}^{-1}$  and 1500  $\text{cm}^{-1}$  to 1400  $\text{cm}^{-1}$  [34,35]. At the same time, the other aromatic stretching mode of C-N bands in the side chains always occurs with the other aromatic stretching bands and bending modes together. Thus, it is hard to separate the modes between them. The N-H stretching modes have been found at a high level. In the literature, the C-N stretching band has been observed at 1368  $\text{cm}^{-1}$  in benzamide [36].

Moreover, the stretching frequency mode for the C-N bands in the salicylic aldoxime has been recorded at 1617  $\text{cm}^{-1}$ . Similarly, the frequency value of the N-H stretching modes has been observed at 3481  $\text{cm}^{-1}$  in the aniline [37]. In the present study, the C-N stretching vibration bands in the ring-b have appeared at 1759, 1593, 1322, 1308, 1262, 1217, 1186, 1143, and 895  $\text{cm}^{-1}$  at B3LYP/6-311++G(d,p) level of theory.

On the other hand, the related modes have been observed to be about 1862, 1666, 1415, 1368, 1255, 1226, 1195, 1168, and 947  $\text{cm}^{-1}$  at HF/6-311++G(d,p) basis set. The experimentally observed C-N stretching vibration bands have been found at 1720, 1687, 1630, 1249, 1236, 1186, and 1141  $\text{cm}^{-1}$ . The C-N stretching vibration modes have been obtained at about 1086, 1076, 982, and 583  $\text{cm}^{-1}$  at B3LYP/6-311++G(d,p) calculation level while the modes have been observed to be in a range of 1116, 1107, 1006, and 606  $\text{cm}^{-1}$  at HF/6-311++G(d,p) basis set. The observed mode has been measured to be about 968  $\text{cm}^{-1}$  for the N-(4-dimethylamino 3,5-dinitrophenyl)maleimide compound. At the same time, the other aromatic nitro compounds with asymmetric and symmetric stretching vibrational bands have been detected to be strong absorptions at 1485-1570  $\text{cm}^{-1}$  [38] and 1320-1370  $\text{cm}^{-1}$  [39], respectively. Likewise, the NO stretching vibrational modes are in a range of 1340-1450  $\text{cm}^{-1}$  [40]. In the current work, the NO stretching vibrational modes have been calculated to be in a range of 1524-762  $\text{cm}^{-1}$  at B3LYP/6-311++G(d,p) calculation level, while the modes have been observed to be in a range of 1625-821  $\text{cm}^{-1}$  at HF/6-311++G(d,p) basis set.

As for the appearance of bending modes in the compound, the C-H bending vibrational modes in the ring-a have been calculated between 1706-541  $\text{cm}^{-1}$  for the CCH bending vibrational modes at B3LYP/6-311++G(d,p) calculation level, whereas the modes have been determined to be in a range from 1798  $\text{cm}^{-1}$  to 556  $\text{cm}^{-1}$ . In ring-b, the mode values intervals of 1524-392  $\text{cm}^{-1}$  and 1625-396  $\text{cm}^{-1}$  have been observed at B3LYP/6-311++G(d,p) and HF/6-311++G(d,p) basis sets. The other bending modes (rocking, torsion, umbrella, breathing, wagging, scissoring, and twisting) have been provided in Tables 2 and 3.

**Table 1.** Calculated DFT (cm<sup>-1</sup>) frequencies and Experimental frequencies (cm<sup>-1</sup>)

Assignments	Scaled Freq. (cm <sup>-1</sup> )	Red. Masses	Frc Consts	IR Intent	Raman Actv	Depolar (P)	Depolar (U)	Exp. Freq.
$\nu_{\text{sym}}^{\text{a}}(\text{CH})$	3114	1.1090	6.9036	0.26	247.14	0.1573	0.2719	3107
$\nu_{\text{asym}}^{\text{b}}(\text{CH})$	3096	1.0916	6.7205	14.14	24.69	0.7500	0.8571	
$\nu_{\text{sym}}^{\text{b}}(\text{CH})$	3095	1.0926	6.7244	0.075	46.97	0.0985	0.1793	3095
$\nu_{\text{asym}}^{\text{a}}(\text{CH})$	3094	1.0894	6.6967	0.15	119.63	0.7500	0.8571	3082
$\nu_{\text{asym}}(\text{CH}_3)$	2996	1.1005	6.3421	13.06	57.45	0.7137	0.8329	
$\nu_{\text{asym}}(\text{CH}_3)$	2995	1.1003	6.3357	5.7304	9.89	0.7500	0.8571	
$\nu_{\text{asym}}(\text{CH}_3)$	2944	1.1053	6.1500	1.1152	43.06	0.6040	0.7531	2964
$\nu_{\text{asym}}(\text{CH}_3)$	2939	1.1043	6.1255	35.4097	193.68	0.7500	0.8571	2924
$\nu_{\text{sym}}(\text{CH}_3)$	2894	1.0357	5.5697	80.6611	517.00	0.0681	0.1275	
$\nu_{\text{sym}}(\text{CH}_3)$	2887	1.0349	5.5422	31.2089	45.81	0.7500	0.8571	
$\nu_{\text{sym}}(\text{C}=\text{O}_2) + \nu^{\text{b}}(\text{N}-\text{C})$	1759	12.4075	24.6547	0.5709	96.65	0.1764	0.2998	1720
$\nu_{\text{sym}}(\text{C}=\text{O}_2) + \gamma^{\text{a}}(\text{CCH})$	1706	12.4507	23.2754	626.4407	0.3024	0.7500	0.8571	1706
$\nu^{\text{b}}(\text{C}=\text{C}) + \gamma^{\text{a}}(\text{CCH}) + \gamma^{\text{a}}(\text{CCH}) + \nu^{\text{b}}(\text{N}-\text{C})$	1593	7.1938	11.7271	107.8010	171.9320	0.5392	0.7006	1687-1630
$\nu^{\text{a}}(\text{C}=\text{C}) + \gamma^{\text{a}}(\text{CCH}) +$	1576	6.7274	10.7352	5.0778	42.4942	0.0442	0.0847	1543
$\nu(\text{N}=\text{O}) + \nu^{\text{a}}(\text{C}=\text{C}) + \phi^{\text{b}}(\text{CH}_3) + \gamma^{\text{b}}(\text{CCH})$	1524	12.0810	18.0348	290.6978	2.7197	0.7500	0.8571	1528
$\nu(\text{N}=\text{O}) + \nu^{\text{a}}(\text{C}=\text{C}) + \phi^{\text{b}}(\text{CCH})$	1522	8.8722	13.2033	383.6740	123.2386	0.4850	0.6532	
$\nu^{\text{b}}(\text{C}=\text{C}) + \nu^{\text{b}}(\text{CCH})$	1503	8.2232	11.9412	61.1878	7.6190	0.7500	0.8571	
$\nu(\text{N}=\text{O}) + 3^{\text{b}}(\text{CCH})$	1494	2.2320	3.1986	153.7839	2.4706	0.7439	0.8532	
$\nu(\text{N}=\text{O}) + 3^{\text{b}}(\text{CH}_3)$	1444	1.2150	1.6276	3.3154	49.1572	0.4239	0.5954	1468
$3^{\text{b}}(\text{CH}_3)$	1439	1.0602	1.4102	25.9684	2.2021	0.7500	0.8571	1438
$3^{\text{b}}(\text{CH}_3)$	1434	1.0472	1.3832	26.1861	1.9936	0.7500	0.8571	
$3^{\text{b}}(\text{CCH})$	1427	1.1043	1.4448	5.8453	12.9432	0.5427	0.7036	1422
$\nu(\text{N}=\text{O}) + 3^{\text{b}}(\text{CH}_3) + \gamma^{\text{b}}(\text{CCH})$	1401	1.6170	2.0368	200.3489	29.4370	0.1697	0.2902	
$\nu^{\text{b}}(\text{CH}_3) + \nu(\text{N}=\text{O}) + \gamma^{\text{b}}(\text{CCH})$	1390	1.1396	1.4148	0.2550	10.7982	0.7500	0.8571	
$\nu^{\text{b}}(\text{C}=\text{C}) + \gamma^{\text{b}}(\text{CCH})$	1381	3.8179	4.6800	16.3654	2.8174	0.7500	0.8571	1377
$\gamma^{\text{b}}(\text{CCH}) + \nu(\text{N}=\text{O}) + 3^{\text{b}}(\text{CH}_3) + \nu^{\text{b}}(\text{N}-\text{C})$	1370	4.5152	5.4442	70.2034	38.2015	0.4091	0.5807	1366
$\nu(\text{N}=\text{O}) + \nu^{\text{b}}(\text{C}=\text{C}) + \gamma^{\text{b}}(\text{CCH})$	1322	3.7628	4.2226	281.3185	133.9973	0.2659	0.4200	
$\nu(\text{N}=\text{O}) + \nu^{\text{b}}(\text{C}=\text{C}) + \gamma^{\text{b}}(\text{CCH})$	1313	11.0749	12.2675	344.0675	13.8591	0.7500	0.8571	
$\nu(\text{N}=\text{O}) + \nu^{\text{b}}(\text{N}-\text{C}) + \gamma^{\text{b}}(\text{CCH})$	1308	9.2975	10.2110	42.9441	237.6281	0.1569	0.2712	
$\gamma^{\text{b}}(\text{CCH}) + \nu^{\text{b}}(\text{C}=\text{C})$	1271	1.9399	2.0131	10.6930	11.9878	0.7500	0.8571	1284
$\gamma^{\text{a}}(\text{CCH}) + \nu^{\text{b}}(\text{C}=\text{C}) + \nu(\text{CH}_3) + \nu^{\text{b}}(\text{N}-\text{C})$	1262	6.6373	6.7889	135.4079	17.9333	0.7500	0.8571	1249-1236
$\gamma^{\text{b}}(\text{CCH}) + \nu^{\text{b}}(\text{N}-\text{C}) + \nu(\text{CH}_3)$	1217	2.2041	2.0975	77.9363	1.6895	0.7500	0.8571	
$\text{B}^{\text{b}} + \phi^{\text{b}}(\text{CCH}) + \nu^{\text{b}}(\text{N}-\text{C}) + \nu^{\text{a}}(\text{C}=\text{C})$	1186	4.5375	4.1027	75.8744	49.1308	0.2579	0.4101	1186
$\nu^{\text{b}}(\text{C}=\text{C}) + \nu^{\text{b}}(\text{CCH}) + \nu(\text{CH}_3)$	1152	2.3175	1.9734	5.2908	0.2270	0.7500	0.8571	1177
$\nu(\text{CH}_3) + \nu^{\text{b}}(\text{N}-\text{C}) + 3^{\text{b}}(\text{CCH})$	1143	1.7769	1.4902	31.5136	15.1952	0.2222	0.3637	1141
$\nu(\text{CH}_3) + \gamma^{\text{b}}(\text{CCH})$	1103	1.4077	1.0998	5.5543	1.0360	0.7500	0.8571	1113
$\nu^{\text{a}}(\text{N}-\text{C}) + \nu^{\text{b}}(\text{CCH}) + \gamma^{\text{b}}(\text{CCH})$	1086	6.5545	4.9742	89.6597	11.8526	0.7500	0.8571	
$\nu(\text{CH}_3) + \gamma^{\text{b}}(\text{CCC}) + 3^{\text{b}}(\text{CCH}) + \nu^{\text{a}}(\text{N}-\text{C}) + 3^{\text{b}}(\text{CCH})$	1078	2.1844	1.6303	42.6011	7.4200	0.6129	0.7600	1076
$\nu(\text{CH}_3) + \gamma^{\text{b}}(\text{CCH})$	1071	1.2712	0.9375	2.0055	3.5920	0.6971	0.8215	
$3^{\text{a}}(\text{CCH}) + 3^{\text{b}}(\text{CCH}) + \nu^{\text{b}}(\text{C}=\text{C})$	1044	1.3026	0.9125	23.3185	25.6504	0.1849	0.3121	
$\nu(\text{CH}_3)$	1041	1.4899	1.0377	9.6567	0.5869	0.7500	0.8571	1036
$\gamma^{\text{b}}(\text{CCH}) + 3^{\text{a}}(\text{CCH}) + \gamma^{\text{a}}(\text{CNC}) + \nu^{\text{a}}(\text{C}=\text{C})$	1002	3.8530	2.4870	8.4983	1.0230	0.7500	0.8571	
$\text{B}^{\text{a}} + \nu^{\text{a}}(\text{N}-\text{C}) + \nu^{\text{b}}(\text{C}=\text{C}) + 3^{\text{a}}(\text{CCH})$	982	3.7321	2.3118	6.2692	4.6071	0.5477	0.7078	968
$\phi^{\text{a}}(\text{CCH})$	936	1.2982	0.7310	0.0087	1.0154	0.5589	0.7171	
$\text{B}^{\text{b}} + \nu(\text{CH}_3)$	931	3.3876	1.8884	36.3164	23.2198	0.3018	0.4637	926

$\nu$ , stretching;  $\gamma$ , bending;  $\nu$ , rocking;  $\psi$ , torsion; U, umbrella; B, breathing; w, wagging; asy, asymmetric; sym, symmetric; 3, scissoring;  $\phi$ , twisting.  
a - Ring1. b - Ring2

Table 1. Continued

Assignments	Scaled Freq. (cm <sup>-1</sup> )	DFT	Red. Masses	Frc Consts	IR Intent	Raman Actv	Depolar (P)	Depolar (U)	Exp. Freq.
$\nu^b(\text{N-C}) + \nu(\text{N=O}) + \gamma^a(\text{CCC}) + \phi^b(\text{CCH})$	895	9.7180	5.0031	45.0523	0.8577	0.7500	0.8571		895
$3^b(\text{CCH})$	874	1.6935	0.8302	20.3834	0.3072	0.7500	0.8571		
<b>B molecule</b>	833	10.8181	4.8175	0.2168	1.1043	0.6400	0.7805		828
$3^a$	810	2.1233	0.8937	59.9978	1.0708	0.7500	0.8571		
$\nu(\text{N=O}) + 3^b(\text{CCH}) + \gamma(\text{CNO}) + \text{B molecule}$	762	7.7001	2.8721	13.2223	0.3576	0.7499	0.8571		777
$\phi^a + \gamma(\text{CNO}) + \gamma^b(\text{CCC}) + \gamma(\text{ONO}) + \phi^a + 3^b(\text{CCH}) + \gamma(\text{ONO}) + \gamma^b(\text{CCC}) + \gamma^b(\text{CCH}) + \gamma^b(\text{CCC}) + \gamma(\text{ONO}) + \gamma^b(\text{CCH})$	738	8.0241	2.8069	3.4473	1.3791	0.7287	0.8431		
$\gamma^b(\text{CCC}) + \gamma(\text{ONO}) + \gamma^b(\text{CCH})$	723	9.4167	3.1638	19.9119	0.4571	0.7500	0.8571		721-714
$\gamma^a(\text{CCC}) + \gamma^a(\text{CNC}) + \text{B molecule}$	693	8.0478	2.4827	16.8113	0.5729	0.7500	0.8571		696
$\phi$ molecule	671	8.0038	2.3171	46.5940	2.2883	0.7500	0.8571		
<b>B molecule</b>	660	6.0232	1.6857	0.3855	1.0092	0.5250	0.6886		
$\phi$ molecule	627	4.8020	1.2108	0.7821	0.4819	0.7500	0.8571		
<b>B molecule</b>	602	10.0988	2.3482	20.9262	14.2229	0.0904	0.1657		
$\phi$ molecule	601	2.4006	0.5576	4.3697	0.2282	0.7476	0.8556		
$\gamma^b(\text{CCH}) + 3^a(\text{CCC}) + \nu^a(\text{N-C}) + \gamma^a(\text{NCO}) + \gamma^b(\text{CCH}) + \gamma^a(\text{CCH}) + \gamma^a(\text{NCO}) + \phi^b + \gamma^b(\text{NCO}) + \gamma(\text{CNC}) + \gamma(\text{CNC}) + \gamma^a(\text{CCO}) + \gamma^a(\text{CCC}) + \gamma^b(\text{CNC}) + w^b + \gamma^a(\text{CNC}) + \gamma(\text{CNO}) + \gamma(\text{CNC}) + \gamma^b(\text{CCH}) + \gamma^a(\text{NCO}) + \gamma(\text{CNC}) + \nu^b$	583	3.8183	0.8356	12.6646	0.4722	0.7500	0.8571		
$\gamma^b(\text{CCH}) + \gamma^a(\text{CCH}) + \gamma^a(\text{NCO}) + \phi^b + \gamma^b(\text{NCO}) + \gamma(\text{CNC}) + \gamma(\text{CNC}) + \gamma^a(\text{CCO}) + \gamma^a(\text{CCC}) + \gamma^b(\text{CNC}) + w^b + \gamma^a(\text{CNC}) + \gamma(\text{CNO}) + \gamma(\text{CNC}) + \gamma^b(\text{CCH}) + \gamma^a(\text{NCO}) + \gamma(\text{CNC}) + \nu^b$	541	3.8823	0.7309	1.9633	0.6887	0.7500	0.8571		
$\phi^b + \gamma^b(\text{NCO}) + \gamma(\text{CNC}) + \gamma(\text{CNC}) + \gamma^a(\text{CCO}) + \gamma^a(\text{CCC}) + \gamma^b(\text{CNC}) + w^b + \gamma^a(\text{CNC}) + \gamma(\text{CNO}) + \gamma(\text{CNC}) + \gamma^b(\text{CCH}) + \gamma^a(\text{NCO}) + \gamma(\text{CNC}) + \nu^b$	521	5.7624	1.0072	5.9953	1.3013	0.2279	0.3712		
$\gamma(\text{CNC}) + \gamma^a(\text{CCO}) + \gamma^a(\text{CCC}) + \gamma^b(\text{CNC}) + w^b + \gamma^a(\text{CNC}) + \gamma(\text{CNO}) + \gamma(\text{CNC}) + \gamma^b(\text{CCH}) + \gamma^a(\text{NCO}) + \gamma(\text{CNC}) + \nu^b$	440	5.6444	0.7035	5.4487	2.2408	0.7200	0.8372		
$\gamma^a(\text{CCC}) + \gamma^b(\text{CNC}) + w^b + \gamma^a(\text{CNC}) + \gamma(\text{CNO}) + \gamma(\text{CNC}) + \gamma^b(\text{CCH}) + \gamma^a(\text{NCO}) + \gamma(\text{CNC}) + \nu^b$	424	7.7694	0.8991	0.0907	0.9860	0.7500	0.8571		
$w^b + \gamma^a(\text{CNC}) + \gamma(\text{CNO}) + \gamma(\text{CNC}) + \gamma^b(\text{CCH}) + \gamma^a(\text{NCO}) + \gamma(\text{CNC}) + \nu^b$	401	8.4488	0.8742	0.6215	0.8359	0.7500	0.8571		
$\gamma(\text{CNC}) + \gamma^b(\text{CCH}) + \gamma^a(\text{NCO}) + \gamma(\text{CNC}) + \nu^b$	392	4.0042	0.3948	22.7896	1.4374	0.2831	0.4412		
$\gamma(\text{CNC}) + \nu^b$	370	5.5737	0.4897	1.3311	0.4771	0.7500	0.8571		
$\gamma(\text{CNC}) + \phi^b + \gamma(\text{CNO}) + \gamma(\text{CNC}) + \gamma^a(\text{CNC}) + \text{B}^b + \gamma^b(\text{CNC}) + \phi^b$	357	4.9990	0.4115	0.0089	7.9951	0.3057	0.4683		
$\gamma(\text{CNC}) + \gamma^a(\text{CNC}) + \text{B}^b + \gamma^b(\text{CNC}) + \phi^b$	333	4.4450	0.3189	1.7528	0.8401	0.7500	0.8571		
$\text{B}^b + \gamma^b(\text{CNC}) + \phi^b$	290	8.7592	0.4765	1.0288	6.7781	0.3453	0.5134		
$\phi^b$	277	4.1273	0.2041	0.0517	1.3244	0.6255	0.7696		
$\psi \text{ CH}_3 + \gamma^b(\text{CNC}) + \psi \text{ CH}_3$	266	1.9291	0.0879	4.2420	0.2989	0.7500	0.8571		
$\psi \text{ CH}_3$	247	1.0796	0.0424	0.0246	2.4677	0.6532	0.7902		
$\text{B}^b + \psi \text{ CH}_3 + \gamma^b(\text{NCO}) + \psi \text{ CH}_3 + \psi \text{ CH}_3 + \gamma^a(\text{NCO}) + \psi \text{ CH}_3 + \gamma^b(\text{NCO}) + \nu \text{ CH}_3 + \gamma^b(\text{NCO}) + \nu^a + \phi^b + \nu \text{ CH}_3 + \nu \text{ molecule} + \nu \text{ molecule} + \nu \text{ CH}_3 + \gamma^b(\text{CCN}) + \nu \text{ NO}_2 + \psi \text{ CH}_3 + \psi^a + w \text{ molecule} + \nu \text{ NO}_2 + \nu \text{ CH}_3 + \phi \text{ molecule} + w \text{ molecule} + w \text{ molecule}$	238	5.4417	0.1976	6.9046	2.1431	0.1432	0.2506		
$\psi \text{ CH}_3 + \psi \text{ CH}_3 + \gamma^a(\text{NCO}) + \psi \text{ CH}_3 + \gamma^b(\text{NCO}) + \nu \text{ CH}_3 + \gamma^b(\text{NCO}) + \nu^a + \phi^b + \nu \text{ CH}_3 + \nu \text{ molecule} + \nu \text{ molecule} + \nu \text{ CH}_3 + \gamma^b(\text{CCN}) + \nu \text{ NO}_2 + \psi \text{ CH}_3 + \psi^a + w \text{ molecule} + \nu \text{ NO}_2 + \nu \text{ CH}_3 + \phi \text{ molecule} + w \text{ molecule} + w \text{ molecule}$	238	3.0142	0.1095	0.0982	0.0925	0.7458	0.8544		
$\psi \text{ CH}_3 + \gamma^a(\text{NCO}) + \psi \text{ CH}_3 + \gamma^b(\text{NCO}) + \nu \text{ CH}_3 + \gamma^b(\text{NCO}) + \nu^a + \phi^b + \nu \text{ CH}_3 + \nu \text{ molecule} + \nu \text{ molecule} + \nu \text{ CH}_3 + \gamma^b(\text{CCN}) + \nu \text{ NO}_2 + \psi \text{ CH}_3 + \psi^a + w \text{ molecule} + \nu \text{ NO}_2 + \nu \text{ CH}_3 + \phi \text{ molecule} + w \text{ molecule} + w \text{ molecule}$	214	4.1046	0.1212	1.4124	1.6448	0.7500	0.8571		
$\psi \text{ CH}_3 + \gamma^b(\text{NCO}) + \nu \text{ CH}_3 + \gamma^b(\text{NCO}) + \nu^a + \phi^b + \nu \text{ CH}_3 + \nu \text{ molecule} + \nu \text{ molecule} + \nu \text{ CH}_3 + \gamma^b(\text{CCN}) + \nu \text{ NO}_2 + \psi \text{ CH}_3 + \psi^a + w \text{ molecule} + \nu \text{ NO}_2 + \nu \text{ CH}_3 + \phi \text{ molecule} + w \text{ molecule} + w \text{ molecule}$	193	3.3394	0.0803	4.8413	0.6067	0.7500	0.8571		
$\nu \text{ CH}_3 + \gamma^b(\text{NCO}) + \nu^a + \phi^b + \nu \text{ CH}_3 + \nu \text{ molecule} + \nu \text{ molecule} + \nu \text{ CH}_3 + \gamma^b(\text{CCN}) + \nu \text{ NO}_2 + \psi \text{ CH}_3 + \psi^a + w \text{ molecule} + \nu \text{ NO}_2 + \nu \text{ CH}_3 + \phi \text{ molecule} + w \text{ molecule} + w \text{ molecule}$	178	7.3127	0.1505	1.0282	3.6784	0.4127	0.5842		
$\phi^b + \nu \text{ CH}_3 + \nu \text{ molecule} + \nu \text{ molecule} + \nu \text{ CH}_3 + \gamma^b(\text{CCN}) + \nu \text{ NO}_2 + \psi \text{ CH}_3 + \psi^a + w \text{ molecule} + \nu \text{ NO}_2 + \nu \text{ CH}_3 + \phi \text{ molecule} + w \text{ molecule} + w \text{ molecule}$	165	5.7984	0.1016	2.0349	5.6968	0.6895	0.8162		
$\nu \text{ molecule} + \nu \text{ molecule} + \nu \text{ CH}_3 + \gamma^b(\text{CCN}) + \nu \text{ NO}_2 + \psi \text{ CH}_3 + \psi^a + w \text{ molecule} + \nu \text{ NO}_2 + \nu \text{ CH}_3 + \phi \text{ molecule} + w \text{ molecule} + w \text{ molecule}$	144	5.2548	0.0700	0.2366	1.7520	0.7500	0.8571		
$\nu \text{ molecule} + \nu \text{ CH}_3 + \gamma^b(\text{CCN}) + \nu \text{ NO}_2 + \psi \text{ CH}_3 + \psi^a + w \text{ molecule} + \nu \text{ NO}_2 + \nu \text{ CH}_3 + \phi \text{ molecule} + w \text{ molecule} + w \text{ molecule}$	121	9.9501	0.0945	9.1175	0.2971	0.7500	0.8571		
$\nu \text{ CH}_3 + \gamma^b(\text{CCN}) + \nu \text{ NO}_2 + \psi \text{ CH}_3 + \psi^a + w \text{ molecule} + \nu \text{ NO}_2 + \nu \text{ CH}_3 + \phi \text{ molecule} + w \text{ molecule} + w \text{ molecule}$	106	4.2305	0.0311	10.1937	3.6734	0.5847	0.7380		
$\nu \text{ NO}_2 + \psi \text{ CH}_3 + \psi^a + w \text{ molecule} + \nu \text{ NO}_2 + \nu \text{ CH}_3 + \phi \text{ molecule} + w \text{ molecule} + w \text{ molecule}$	71	9.5781	0.0316	0.9047	2.4715	0.7500	0.8571		
$w \text{ molecule} + \nu \text{ NO}_2 + \nu \text{ CH}_3 + \phi \text{ molecule} + w \text{ molecule} + w \text{ molecule}$	70	6.5069	0.0205	4.2314	0.5583	0.7500	0.8571		
$\nu \text{ NO}_2 + \nu \text{ CH}_3 + \phi \text{ molecule} + w \text{ molecule} + w \text{ molecule}$	69	8.9288	0.0276	0.2660	3.4854	0.5551	0.7139		
$\phi \text{ molecule} + w \text{ molecule} + w \text{ molecule}$	62	8.0780	0.0206	0.2173	0.6891	0.7500	0.8571		
$w \text{ molecule} + w \text{ molecule}$	36	6.0630	0.0054	3.3309	1.2818	0.7500	0.8571		
$w \text{ molecule}$	24	11.7827	0.0045	0.2885	4.1201	0.7242	0.8400		

$\nu$ , stretching;  $\gamma$ , bending;  $\nu$ , rocking;  $\psi$ , torsion; U, umbrella; B, breathing; w, wagging; asy, asymmetric; sym, symmetric; 3, scissoring;  $\phi$ , twisting. a - Ring1. b - Ring2

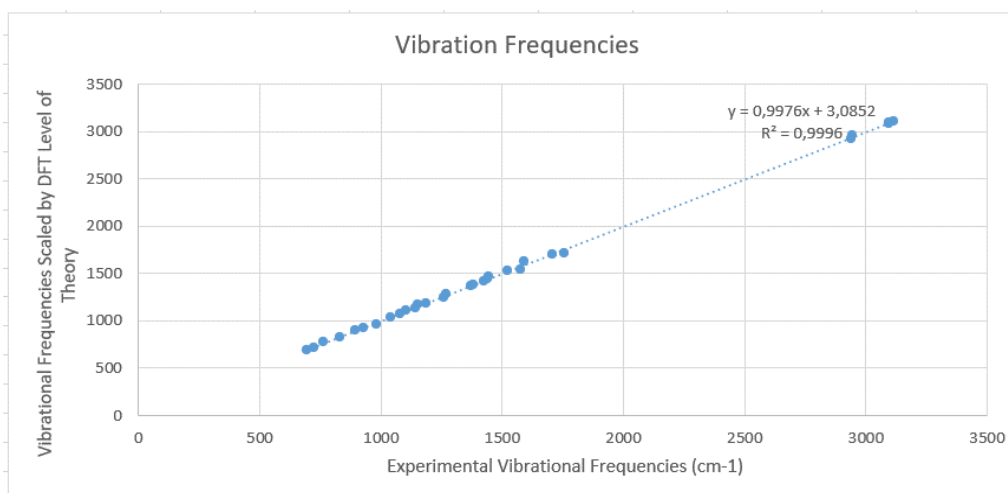


**Figure 2.** Change of vibrational frequencies scaled by DFT-B3LYP/6–311++G(d,p) basis set versus experimental vibrational frequencies

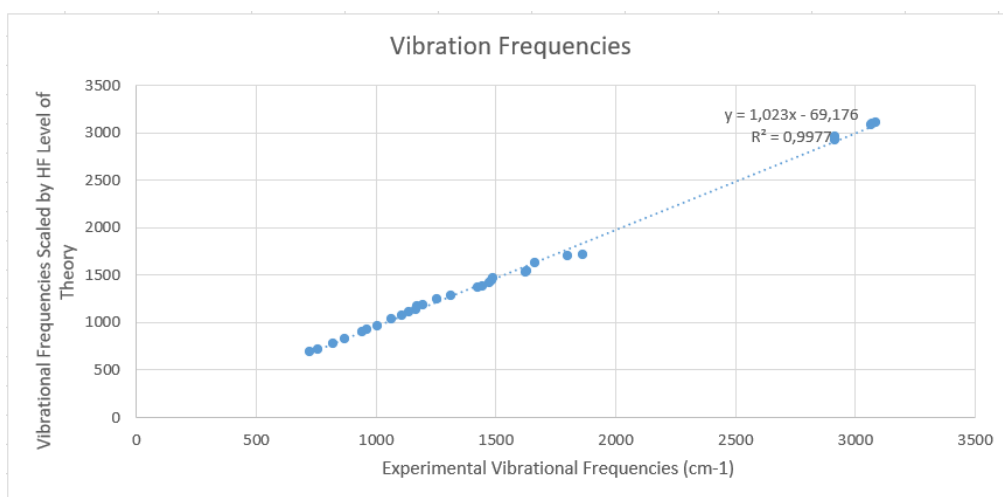


**Figure 3.** Change of vibrational frequencies scaled by HF-B3LYP/6–311++G(d,p) basis set versus experimental vibrational frequencies

**Table 2.** Calculated HF frequencies (cm<sup>-1</sup>) and Experimental frequencies (cm<sup>-1</sup>)

Assignments	Scaled Freq. (cm <sup>-1</sup> ) HF	Red. Masses	Frc Consts	IR Intent	Raman Actv	Depolar (P)	Depolar (U)	Exp. Freq.
$\nu_{\text{sym}}^{\text{a}}(\text{CH})$	3086	1.11	7.62	0.48	173.47	0.1614	0.2779	3107
$\nu_{\text{asym}}^{\text{b}}(\text{CH})$	3070	1.09	7.42	9.26	26.20	0.7500	0.8571	
$\nu_{\text{sym}}^{\text{b}}(\text{CH})$	3070	1.09	7.42	0.05	60.54	0.1128	0.2027	3095
$\nu_{\text{asym}}^{\text{a}}(\text{CH})$	3066	1.09	7.38	0.46	87.92	0.7500	0.8571	3082
$\nu_{\text{asym}}(\text{CH}_3)$	2956	1.10	6.93	35.1349	42.38	0.7441	0.8533	
$\nu_{\text{asym}}(\text{CH}_3)$	2954	1.10	6.9237	9.1717	16.94	0.7500	0.8571	
$\nu_{\text{asym}}(\text{CH}_3)$	2916	1.1050	6.7596	0.3324	19.43	0.7475	0.8555	2964
$\nu_{\text{asym}}(\text{CH}_3)$	2914	1.1043	6.7461	56.3837	148.90	0.7500	0.8571	2924
$\nu_{\text{sym}}(\text{CH}_3)$	2868	1.0363	6.1327	88.0587	349.09	0.0360	0.0695	

$\nu$ , stretching;  $\gamma$ , bending;  $\rho$ , rocking;  $\psi$ , torsion; U, umbrella; B, breathing; w, wagging; asy, asymmetric; sym, symmetric; 3, scissoring;  $\phi$ , twisting.  
a - Ring1. b - Ring2

Table 2. Continued

Assignments	Scaled Freq. (cm <sup>-1</sup> ) HF	Red. Masses	Frc Consts	IR Intent	Raman Actv	Depolar (P)	Depolar (U)	Exp. Freq.
$\nu_{\text{sym}}(\text{CH}_3)$	2862	1.0352	6.1005	39.8838	23.9361	0.7500	0.8571	
$\nu_{\text{sym}}(\text{C}=\text{O}_2) + \nu^b(\text{N}-\text{C})$	1862	12.2950	30.6740	6.6877	91.8958	0.2750	0.4314	1720
$\nu_{\text{sym}}(\text{C}=\text{O}_2) + \gamma^a(\text{CCH})$	1798	12.4815	29.0102	1003.7862	2.9709	0.7500	0.8571	1706
$\nu^b(\text{C}=\text{C}) + \gamma^a(\text{CCH}) + \gamma^a(\text{CCH}) + \nu^b(\text{N}-\text{C})$	1666	9.2170	18.4192	372.0050	73.0194	0.5446	0.7052	1687-1630
$\nu^a(\text{C}=\text{C}) + \gamma^a(\text{CCH}) +$	1632	13.7990	26.4563	747.5561	1.2899	0.7500	0.8571	1543
$\nu(\text{N}=\text{O}) + \nu^a(\text{C}=\text{C}) + \phi^b(\text{CH}_3) + \gamma^b(\text{CCH})$	1625	6.6719	12.6709	1.1724	61.8098	0.0597	0.1127	1528
$\nu(\text{N}=\text{O}) + \nu^a(\text{C}=\text{C}) + \phi^b(\text{CCH})$	1614	7.4546	13.9700	275.9697	105.3286	0.4830	0.6514	
$\nu^b(\text{C}=\text{C}) + \nu^b(\text{CCH})$	1575	7.8892	14.0733	29.5236	3.1870	0.7500	0.8571	
$\nu(\text{N}=\text{O}) + 3^b(\text{CCH})$	1524	2.0656	3.4516	307.5915	29.8872	0.3457	0.5138	
$\nu(\text{N}=\text{O}) + 3^b(\text{CH}_3)$	1487	10.0456	15.9799	42.8994	55.0893	0.0481	0.0917	1468
$3^b(\text{CH}_3)$	1483	4.8848	7.7303	372.9556	5.1759	0.7500	0.8571	1438
$3^b(\text{CH}_3)$	1479	1.3330	2.0975	22.2763	10.6868	0.7494	0.8568	
$3^b(\text{CCH})$	1475	1.1940	1.8698	33.5022	1.1377	0.7500	0.8571	1422
$\nu(\text{N}=\text{O}) + 3^b(\text{CH}_3) + \gamma^b(\text{CCH})$	1464	1.0651	1.6419	15.7372	2.0592	0.7500	0.8571	
$\nu^b(\text{CH}_3) + \nu(\text{N}=\text{O}) + \gamma^b(\text{CCH})$	1455	1.0875	1.6582	9.0041	8.8913	0.7422	0.8520	
$\nu(\text{CH}_3)$	1443	1.6317	2.4441	236.6356	2.5748	0.7313	0.8448	1377
$\nu^b(\text{C}=\text{C}) + \gamma^b(\text{CCH})$	1426	1.1492	1.6825	1.0932	4.1266	0.7500	0.8571	1366
$\gamma^b(\text{CCH}) + \nu(\text{N}=\text{O}) + 3^b(\text{CH}_3) + \nu^b(\text{N}-\text{C})$	1415	4.6407	6.6877	130.3512	55.8562	0.1369	0.2408	
$\nu(\text{N}=\text{O}) + \nu^b(\text{C}=\text{C}) + \gamma^b(\text{CCH})$	1412	3.7955	5.4482	17.6801	0.8523	0.7500	0.8571	
$\nu(\text{N}=\text{O}) + \nu^b(\text{N}-\text{C}) + \gamma^b(\text{CCH})$	1368	3.1122	4.1865	197.0477	2.7153	0.6981	0.8222	
$\gamma^b(\text{CCH}) + \nu^b(\text{C}=\text{C})$	1312	1.8811	2.3328	0.1565	6.6644	0.7500	0.8571	1284
$\gamma^a(\text{CCH}) + \nu^b(\text{C}=\text{C}) + \nu(\text{CH}_3) + \nu^b(\text{N}-\text{C})$	1255	2.7401	3.1091	36.1686	0.3614	0.7500	0.8571	1249-1236
$\gamma^b(\text{CCH}) + \nu^b(\text{N}-\text{C}) + \nu(\text{CH}_3)$	1226	6.0448	6.5427	77.4441	25.0864	0.3527	0.5215	
$\text{B}^b + \phi^b(\text{CCH}) + \nu^b(\text{N}-\text{C}) + \nu^a(\text{C}=\text{C})$	1195	2.0472	2.1026	1.7835	0.6503	0.7500	0.8571	1186
$\nu^b(\text{C}=\text{C}) + \nu^b(\text{CCH}) + \nu(\text{CH}_3)$	1174	6.2008	6.1463	100.6400	5.1897	0.7500	0.8571	1177
$\nu(\text{CH}_3) + \nu^b(\text{N}-\text{C}) + 3^b(\text{CCH})$	1168	1.7032	1.6716	22.1894	8.0361	0.0529	0.1005	1141
$\nu(\text{CH}_3) + \gamma^b(\text{CCH})$	1139	1.4304	1.3352	17.4903	4.4130	0.7500	0.8571	1113
$\nu^a(\text{N}-\text{C}) + \nu^b(\text{CCH}) + \gamma^b(\text{CCH})$	1116	2.4559	2.2002	51.3000	9.9660	0.3025	0.4645	
$\nu(\text{CH}_3) + \gamma^b(\text{CCC}) + 3^b(\text{CCH}) + \nu^a(\text{N}-\text{C}) + 3^b(\text{CCH})$	1107	6.2438	5.5078	56.3981	22.5867	0.7500	0.8571	1076
$\nu(\text{CH}_3) + \gamma^b(\text{CCH})$	1102	1.2098	1.0564	21.6384	7.9686	0.2597	0.4123	
$3^a(\text{CCH}) + 3^b(\text{CCH}) + \nu^b(\text{C}=\text{C})$	1070	1.4413	1.1867	12.1979	2.2950	0.7500	0.8571	
$\nu(\text{CH}_3)$	1065	1.2918	1.0550	22.5989	22.9221	0.1146	0.2057	1036
$\gamma^b(\text{CCH}) + 3^a(\text{CCH}) + \gamma^a(\text{CNC}) + \nu^a(\text{C}=\text{C})$	1034	3.6301	2.7922	7.2123	3.0356	0.7500	0.8571	
$\text{B}^a + \nu^a(\text{N}-\text{C}) + \nu^b(\text{C}=\text{C}) + 3^a(\text{CCH})$	1006	3.3325	2.4265	1.5861	1.7559	0.7496	0.8569	968
$\phi^a(\text{CCH})$	974	1.3039	0.8904	0.0102	3.4268	0.7275	0.8423	
$\text{B}^b + \nu(\text{CH}_3)$	961	1.4420	0.9597	1.4030	0.1001	0.7370	0.8486	926
$\nu^b(\text{N}-\text{C}) + \nu(\text{N}=\text{O}) + \gamma^a(\text{CCC}) +$	947	10.8291	6.9852	33.9465	0.9672	0.7500	0.8571	
$\phi^b(\text{CCH})$	943	3.3106	2.1209	47.3572	6.3296	0.3778	0.5484	895
$3^b(\text{CCH})$	935	1.7125	1.0771	9.2910	0.0980	0.7500	0.8571	
<b>B molecule</b>	871	11.8565	6.4734	0.4415	1.5150	0.1603	0.2762	828
$3^a$	853	2.1866	1.1442	92.9825	0.9381	0.7500	0.8571	
$\nu(\text{N}=\text{O}) + 3^b(\text{CCH}) + \gamma^b(\text{CNO}) +$	821	7.1215	3.4588	8.4321	1.7575	0.7500	0.8571	777
<b>B molecule</b>	799	8.9931	4.1322	0.7956	10.4168	0.2128	0.3510	
$\phi^a + \gamma^b(\text{CNO}) + \gamma^b(\text{CCC}) +$	781	7.6097	3.3399	13.5348	13.0633	0.0105	0.0207	
$\gamma^b(\text{ONO}) + \phi^a + 3^b(\text{CCH}) +$	768	7.9498	3.3809	2.4818	2.9888	0.7044	0.8266	
$\gamma^b(\text{ONO}) + \gamma^b(\text{CCC}) + \gamma^b(\text{CCH}) +$	758	8.8535	3.6709	26.3410	1.2116	0.7500	0.8571	721-714

$\nu$ , stretching;  $\gamma$ , bending;  $\rho$ , rocking;  $\psi$ , torsion; U, umbrella; B, breathing; w, wagging; asy, asymmetric; sym, symmetric; 3, scissoring;  $\phi$ , twisting.  
a - Ring1. b - Ring2

Table 2. Continued

Assignments	Scaled Freq. (cm <sup>-1</sup> ) HF	Red. Masses	Frc Consts	IR Intent	Raman Actv	Depolar (P)	Depolar (U)	Exp. Freq.
$\gamma^b(\text{CCC}) + \gamma(\text{ONO}) + \gamma^b(\text{CCH})$	726	8.8684	3.3641	48.9181	0.5631	0.7500	0.8571	696
$\gamma^a(\text{CCC}) + \gamma^a(\text{CNC}) +$	694	7.4396	2.5812	46.8675	0.6749	0.7500	0.8571	
<b>B molecule</b>	673	6.0625	1.9807	0.3736	0.5984	0.6251	0.7693	
$\phi$ molecule	650	4.0529	1.2328	0.6954	0.7164	0.7500	0.8571	
<b>B molecule</b>	627	2.5884	0.7333	0.7547	0.1638	0.7500	0.8571	
$\phi$ molecule	618	10.1004	2.7791	20.8632	11.2754	0.0621	0.1170	
$\gamma^b(\text{CCH}) + 3^a(\text{CCC}) + \nu^a(\text{N-C}) + \gamma^a(\text{NCO}) +$	606	3.7415	0.9920	15.7006	0.4647	0.7500	0.8571	
$\gamma^b(\text{CCH}) + \gamma^a(\text{CCH}) + \gamma^a(\text{NCO}) +$	556	3.9346	0.8749	1.0464	0.2843	0.7500	0.8571	
$\phi^b + \gamma^b(\text{NCO}) + \gamma(\text{CNC}) +$	541	5.8786	1.2406	4.8111	1.7530	0.1500	0.2609	
$\gamma(\text{CNC}) + \gamma^a(\text{CCO}) +$	449	6.7029	0.9735	19.2378	3.5610	0.5471	0.7073	
$\gamma^a(\text{CCC}) + \gamma^b(\text{CNC}) +$	432	7.8815	1.0600	5.9593	1.4424	0.7500	0.8571	
$w^b + \gamma^a(\text{CNC}) + \gamma(\text{CNO}) +$	418	8.0107	1.0113	1.8791	0.7437	0.7500	0.8571	
$\gamma(\text{CNC}) + \gamma^b(\text{CCH}) + \gamma^a(\text{NCO})$	396	4.1564	0.4698	23.8989	0.2866	0.4405	0.6116	
$\gamma(\text{CNC}) + \nu^b$	374	6.6844	0.6746	1.5637	0.4516	0.7500	0.8571	
$\gamma(\text{CNC}) + \phi^b + \gamma(\text{CNO}) +$	361	4.6053	0.4331	3.2154	5.5912	0.2183	0.3583	
$\gamma(\text{CNC}) + \gamma^a(\text{CNC}) +$	333	4.7764	0.3812	0.3451	0.4837	0.7500	0.8571	
$B^b + \gamma^b(\text{CNC})$	296	8.0882	0.5119	1.8302	3.5527	0.2192	0.3596	
$\phi^b$	283	4.0688	0.2350	0.0000	1.5739	0.7389	0.8498	
$\psi \text{CH}_3 + \gamma^b(\text{CNC})$	255	3.3158	0.1555	3.4999	0.0304	0.7500	0.8571	
$\psi \text{CH}_3$	229	5.9895	0.2276	7.9920	3.0712	0.0914	0.1675	
$B^b + \psi \text{CH}_3 + \gamma^b(\text{NCO})$	229	5.0768	0.1927	0.3671	0.3372	0.7500	0.8571	
$\psi \text{CH}_3 +$	205	1.9021	0.0578	2.7224	0.3291	0.7500	0.8571	
$\psi \text{CH}_3 + \gamma^a(\text{NCO})$	204	1.0952	0.0329	0.0126	0.2490	0.7324	0.8455	
$\psi \text{CH}_3 + \gamma^b(\text{NCO})$	173	5.4882	0.1183	1.8249	4.1414	0.6985	0.8225	3107
$\nu \text{CH}_3 + \gamma^b(\text{NCO}) + \nu^a$	166	7.1187	0.1420	0.7241	2.3864	0.5147	0.6796	
$\phi^b + \nu \text{CH}_3 +$	165	4.7326	0.0932	4.7627	1.6403	0.7500	0.8571	3095
$\nu$ molecule	121	7.9518	0.0842	9.5198	0.2959	0.7500	0.8571	3082
$\nu$ molecule	110	2.9202	0.0257	5.2397	0.5317	0.7500	0.8571	
$\nu \text{CH}_3 + \gamma^b(\text{CCN})$	86	4.0186	0.0215	10.3331	3.8506	0.5126	0.6777	
$\nu \text{NO}_2 + \psi \text{CH}_3 + \psi^a$	68	10.1695	0.0339	0.3789	1.3397	0.7500	0.8571	2964
<b>w molecule</b>	67	7.3680	0.0242	0.8278	1.7221	0.7340	0.8466	
$\nu \text{NO}_2 + \nu \text{CH}_3$	64	6.4184	0.0192	2.9143	0.4785	0.7500	0.8571	
$\phi$ molecule	61	7.1761	0.0192	0.5392	0.6427	0.7500	0.8571	
<b>w molecule</b>	42	5.7046	0.0071	2.7198	1.2168	0.7500	0.8571	
<b>w molecule</b>	20	11.8775	0.0035	0.2638	3.5809	0.7494	0.8568	

$\nu$ , stretching;  $\gamma$ , bending;  $\nu$ , rocking;  $\psi$ , torsion; U, umbrella; B, breathing; w, wagging; asy, asymmetric; sym, symmetric; 3, scissoring;  $\phi$ , twisting. a - Ring1. b - Ring2

The good agreement between the calculation levels of B3LYP/6-311++G(d,p) and HF/6-311++G(d,p) for the vibrational frequency bands has enabled us to determine the molecular geometric characteristics for the N-(4-dimethylamino 3,5-dinitrophenyl)maleimide. In this respect, the selected molecular geometric features, including some selected bond lengths, bond angles, and dihedrals, have extensively been examined in detail by means of both the B3LYP/6-311++G(d,p) and HF/6-311++G(d,p) levels of theories and determined the correlation between the calculation levels to identify the molecular geometric parameters. One can see the atomic numbered N-(4-dimethylamino 3,5-dinitrophenyl)maleimide compound in Figure 1.

Besides, we have numerically depicted some selected molecular geometric features in Table 3. The bond lengths between the carbon atoms have been calculated to be about 1.39-1.50 Å and 1.38-1.50 Å at the B3LYP/6-311++G(d,p) and HF/6-311++G(d,p) levels of theories, respectively. The results obtained show that all the computations have been observed to agree with each other. As for the bond lengths between the nitrogenous and carbon atoms, the B3LYP/6-311++G(d,p) calculation level has displayed the lengths that have been gathered to be between about 1.37-1.49 Å. Similarly, we have computed the lengths between the nitrogenous and carbon atoms in the range of 1.37-1.49 Å at the HF/6-311++G(d,p) level of theory.

Moreover, the bond lengths between the carbon and hydrogen atoms have been calculated to vary from about 1.08 Å to 1.09 Å at the B3LYP/6-311++G(d,p) level of calculation whereas we have found between 1.07 Å and 1.08 Å for the bond distance values by using the HF/6-311++G(d,p) level of theory. The bond distance between the nitrogenous and oxygen has also been computed to be about 1.23 Å and 1.19 Å at the B3LYP/6-311++G(d,p) and HF/6-311++G(d,p) basis sets, respectively. Moreover, the bond angles and bond dihedrals are in good agreement with each other (see Table 3). There seemed to be some differences in the calculations performed by the B3LYP/6-311++G(d,p) and HF/6-311++G(d,p) levels of calculations due to the conjugation of  $\pi$  existing in both rings, different spatial electron (non-bonding lone pairs) distributions over the bonds in the molecule, and electron-withdrawing strength of high electronegative atoms. Besides, the electron density (electronegative, and electron-acceptor ability characteristics) delocalization, repulsive forces formation between positive or negative charged atoms, inhomogeneous charge distribution, and especially intra-molecular charge transfer (ICT) have led to vary the values of calculation models [41-46].

**Table 3.** Molecular geometric features of the compound

Bond Length(Å)	DFT		Bond Angle(°)	DFT		Bond Dihedrals(°)	DFT	
	HF	B3LYP		HF	B3LYP		HF	B3LYP
<b>C1-C6</b>	1.39	1.38	C1-C2-C3	120.02	119.82	C1-C2-H7-N18	0.75	0.42
<b>C1-N18</b>	1.42	1.42	C1-C2-H7	121.12	120.91	H7-C2-C3-N10	-7.52	-5.31
<b>C6-H8</b>	1.08	1.07	C1-N18-C15	125.07	124.80	C3-C4-N9-O26	38.20	47.27
<b>C3-N10</b>	1.48	1.47	C1-N18-C12	125.07	124.80	C4-N9-C25-H32	13.93	
<b>N10-O24</b>	1.23	1.19	C12-N18-C15	109.85	110.40	O19-C12-N18-C15	179.86	179.50
<b>C4-N9</b>	1.37	1.37	C14-C15-O20	128.08	128.04	N18-C15-C14-H17	-179.88	-179.88
<b>N9-C25</b>	1.46	1.45	C13-C14-H17	129.48	121.60	C4-N9-C26-H28	-107.95	-113.20
<b>C26-H28</b>	1.09	1.08	C6-C5-N11	114.42	114.88	C4-N9-C25-H31	131.61	
<b>C5-N11</b>	1.49	1.47	C5-N11-O21	117.77	117.89	N9-C4-C3-N10	9.19	
<b>C1-N18</b>	1.42	1.42	C4-N9-C25	122.65	122.12	C3-C2-C1-N18	-177.33	-177.58
<b>N18-C15</b>	1.41	1.39	N9-C26-H28	112.05	111.71	C1-N18-C15-C14	-179.98	179.97
<b>C15-O20</b>	1.21	1.18				C1-C4-N9-C25	110.89	54.79
<b>C12-C13</b>	1.50	1.50				C1-C4-N9-C26	-69.12	-125.21

In the present work, the distribution of atomic charges for the N-(4-dimethylamino 3,5-dinitrophenyl)maleimide have been calculated by the Mulliken method [47,48] at the HF/6-311++G(d,p) and B3LYP/6-311++G(d,p) levels of calculation and all the computations for the atoms over the title molecule have been shown in Table 4. It has been observed that the magnitudes pertaining to the carbon atomic charges for the Mulliken calculation method are either positive or negative at the HF/6-311++G(d,p) and B3LYP/6-311++G(d,p) basis sets. These magnitudes have been noted to change between -1.25 and 0.26 for B3LYP/6-311++G(d,p) levels of calculation and between -0.57 and 0.22 for HF/6-311++G(d,p) levels of calculation. The magnitudes of charges calculated on N atoms excluding N28, decrease from HF to DFT calculation level. These values have been found to be 0.06 (N9), -0.39 (N10), -0.24 (N11), 0.44 (N18) at the B3LYP/6-311++G(d,p), and 0.29 (N9), -0.17 (N10), -0.17 (N11), 0.23 (N18) at the HF/6-31G(d,p) levels of calculations.

For O atoms, the magnitude of the charge is either positive or negative at the used basis sets. These magnitudes have been recorded to vary between -0.24 and 0.19 for the B3LYP/6-311++G(d,p) calculation and between -0.33 and 0.03 for the HF/6-311++G(d,p) level of theory. The magnitudes of charges calculated on O atoms have been detected to increase from the HF to DFT levels of calculations. In addition, the magnitudes of the hydrogen atomic charges have been observed to arrange from 0.12 to 0.30. The charge on H8 connected with C6 has been noticed to be the maximum magnitude (0.29 at the B3LYP/6-311++G(d,p) and 0.30 at the HF/6-311++G(d,p) levels of calculation). Although there seems to be a difference between the calculations performed by the HF/6-311++G(d,p) and B3LYP/6-311++G(d,p) basis set due to the presence of conjugation of  $\pi$  existing in both rings, non-bonding lone pairs, inhomogeneous charge distributions, and especially intra-molecular charge transfer in the compound, it has been obvious that there has appeared a good agreement between the calculations.

The NMR examination is another identification study for organic compounds. There is a difference in the calculations performed by the HF/6-311++G(d,p) and B3LYP/6-311++G(d,p) calculation levels for the  $^{13}\text{C}$ -NMR and  $^1\text{H}$ -NMR spectra because of the electron correlations. In more detail, no electron correlation effects have disappeared in the former method; however, in the latter calculation technique, the electronic energy has been treated as a function of the electron density of all electrons simultaneously, and thus the electron correlation effect has been taken in account for the calculations [49].

**Table 4:** Atomic charges for optimized geometry of N-(4-dimethylamino 3,5-dinitrophenyl)maleimide

Label	DFT(B3LYP/6-311++(d,p))	HF (6-311++(d,p))
C1	-1.25	-0.57
C2	0.26	-0.28
C3	0.02	0.21
C4	0.09	-0.41
C5	0.13	0.21
C6	-0.18	-0.28
H7	0.26	0.30
H8	0.29	0.30
N9	0.06	0.29
N10	-0.39	-0.17
N11	-0.24	-0.17
C12	-0.30	0.11
C13	0.13	-0.09
C14	0.06	-0.09
C15	-0.03	0.11
H16	0.23	0.28
H17	0.24	0.28
N18	0.44	0.23
O19	-0.20	-0.33
O20	-0.24	-0.33
O21	0.19	0.03
O22	0.18	0.03
O23	0.02	-0.01
O24	0.11	-0.01
C25	-0.69	-0.36
C26	-0.27	0.22
H27	0.24	0.16
H28	0.12	0.16
H29	0.12	0.16
H30	0.23	0.22
H31	0.17	0.16
H32	0.17	0.16

In this study, the GIAO  $^{13}\text{C}$  and  $^1\text{H}$  NMR chemical shifts of N-(4-dimethylamino 3,5-dinitrophenyl)maleimide have been calculated in the chloroform, and the obtained computations have numerically been depicted in Table 5. As for the comparison to the experimental results, the calculations performed at the B3LYP/6-311++G(d,p) calculation levels for the optimized geometry have been observed to be in good agreement with experimental results [16].  $^1\text{H}$  isotropic chemical shift values have been observed experimentally at 2.84–7.98 parts per million(ppm). On the other hand, the values have been calculated to be in the range of 0.41–7.41 ppm. At the same time, as seen in Table 5, all computations have been in good agreement with experimental data.

The CH proton (H8), observed to be about 7.98 ppm, is 7.13 ppm at the B3LYP/6-311++G(d,p)//HF/6-31G(d) calculation level and 7.41 ppm at B3LYP/6-311++G(d,p)//B3LYP/6-311+G(2d,p) level of theory. However, the chemical shift for the H13 atom has been obtained in good agreement with the experiment. In addition,  $^{13}\text{C}$  chemical shifts concerning TMS calculated at the same basis sets have been given in the same table.  $^{13}\text{C}$  chemical shift values were obtained at 51.2–165.0 ppm, whereas these values were experimentally observed at 42.3–168.2 ppm. The chemical shifts of C12 and C15 have been observed to be 168.2 ppm, whereas they have been noted to be at 155.8 ppm and 165.0 ppm at B3LYP/6-311++G(d,p)//HF/6-31G(d) and B3LYP/6-311++G(d,p)//B3LYP/6-311+G(2d,p) levels of theory, respectively. Nevertheless, the observed shift of C4 was noticed to be more different than the calculated ones because of the effect of chloroform solution on the compound.

**Table 5.**  $^{13}\text{C}$  and  $^1\text{H}$  isotropic chemical shifts (concerning TMS, all values in ppm) for N-(4-dimethylamino 3,5-dinitrophenyl)maleimide

Calculated Chemical Shift(ppm)	In $\text{CDCl}_3$			
	DFT-B3LYP/6-311++G(d,p)	HF/6-311++G(d,p)	Experimental Value	
Carbon Atoms	C12	165.0	155.8	168.2
	C15	163.0	155.8	168.2
	C4	159.0	134.6	138.6
	C13	149.7	124.7	134.6
	C14	148.9	124.7	134.6
	C5	145.7	130.8	145.4
	C3	144.2	130.8	145.4
	C6	143.7	125.9	126.0
	C1	137.6	106.3	123.8
	C2	128.4	125.9	126.0
	C25	56.6	51.2	42.3
	C26	42.0	36.4	42.3
Hydrogen Atoms	H27	3.57	4.63	2.84
	H8	7.41	7.13	7.98
	H16	7.01	5.95	6.92
	H17	6.85	5.95	6.92
	H7	6.07	7.13	7.98
	H30	4.46	1.35	2.84
	H32	3.47	1.49	2.84
	H29	1.78	1.49	2.84
	H31	1.71	0.41	2.84
	H28	1.45	0.41	2.84

We have also determined some essential thermodynamics (including the total energy, zero-point energy, rotational constants, dipole moments, and the change in the total entropies such as rotational, vibrational, and translational) features with the aid of the B3LYP/6-311++G(d,p) and HF/6-311++G(d,p) levels of calculations. One can see all the parameters computed in Table 6. Scale factors have been recommended [50] to predict the zero-point vibration energies accurately. Calculations of the HF/6-311++G(d,p) basis set for the energy parameters and rotational constants are the same as the B3LYP/6-311++G(d,p) level of theory. Moreover, HF data are generally smaller than DFT data for the entropy values.

Additionally, we have theoretically defined the frontier orbitals: the highest occupied molecular orbital (HOMO) and lowest unoccupied molecular orbital (LUMO), which play a crucial role in quantum chemistry. The inner frontier orbitals (HOMO) are the outermost orbital containing electrons and tend to give the electrons such as an electron donor. On the other hand, the last frontier orbitals (LUMO) are the innermost orbital containing free places to accept electrons [51]. According to the molecular orbital theory, the interaction between HOMO and LUMO frontier orbitals for a structure is related to the transition state of  $\pi$ - $\pi^*$  type [52]. Therefore, the energy of the HOMO has directly been associated with the ionization potential, while the LUMO energy has been related to the electron affinity.

Besides, the energy difference between HOMO and LUMO orbital is called the band gap energy  $|\Delta E|$ , determining whether the structure is stable [53]. All the calculations about the frontier orbitals have numerically been depicted in Table 6. In addition, 3D plots of the highest occupied molecular orbitals (HOMOs) and lowest unoccupied molecular orbitals (LUMOs) have been shown in Figure 4. According to the energy band gap (translation from HOMO to LUMO) deduced from the B3LYP/6-311++G(d,p) level of calculation, the value of  $|\Delta E|$  has been calculated to be about 0.113 a.u. for the N-(4-dimethylamino 3,5-dinitrophenyl)maleimide molecule while the band gap has been computed to be about 0.366 at the HF/6-311++G(d,p) level of calculation. The highest occupied molecular orbitals have been noted to localize on the title molecule but slightly on ring-1 mainly. On the other hand, the lowest unoccupied molecular orbitals have been observed to localize on the whole molecule mainly. Moreover, the lowest MO Eigenvalue has been determined to be about -0.128 and 0.025(a.u.) at B3LYP/6-311++G(d,p) and HF/6-311++G(d,p) basis sets, respectively. Conversely, the highest MO Eigenvalue has also been found to be -0.241 (a.u.) at B3LYP/6-311++G(d,p) and -0.341 (a.u.) at HF/6-311++G(d,p) calculation levels.

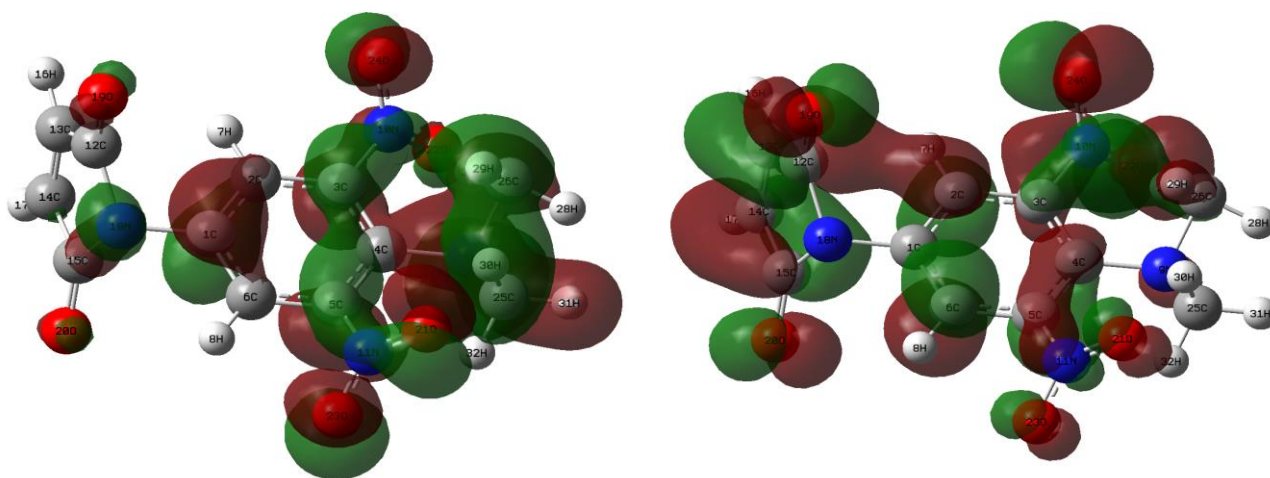


**Figure 4.** 3D plots of (left side) the HOMO and (right side) LUMO of the N-(4-dimethylamino 3,5-dinitrophenyl)maleimide

In this part of the paper, we have focused wholly on the molecular electrostatic potential (MEP) behavior of the N-(4-dimethylamino 3,5-dinitrophenyl)maleimide molecule. It is well known that at any

given point  $r(x, y, z)$  in the vicinity of a molecule, the molecular electrostatic potential  $V(r)$  is defined by the interaction energy between the electrical charge generated from the molecule electrons and nuclei and a positive test charge (a proton) located at  $r$  [54,55]. The molecular electrostatic potential (MEP) is related to the electronic density and is a very useful descriptor for determining sites for electrophilic attack and nucleophilic reactions, as well as hydrogen-bonding interactions [56,57].

**Table 6.** Theoretically computed energies (a.u.), zero-point vibrational energies (kcal mol<sup>-1</sup>), rotational constants (GHz) entropies (cal mol<sup>-1</sup> K<sup>-1</sup>), dipole moment (Debye), and some of the calculated energy values as HOMO, LUMO and  $|\Delta E|$  for N-(4-dimethylamino 3,5-dinitrophenyl)maleimide

Computed Energies		DFT	HF
Parameter	Total Energy	-1133.52	-1126.99
	Zero-point Energy	141.40	152.71
	Rotational Constant	0.43	0.45
		0.21	0.21
0.16		0.16	
Entropy	Total	145.76	143.60
	Translational	43.05	43.05
	Rotational	34.38	34.33
	Vibrational	68.32	66.22
	Dipole Moment	2.48	3.76
Quantity	HOMO	-0.241	-0.341
	LUMO	-0.128	0.025
	$\Delta E$	0.113	0.366

In Figure 5, where negative (red) regions have presented the regions for the electrophilic attack, the regions for the nucleophilic reactivity wave have been displayed by MEP's positive (blue) regions. The figure shows that the red regions of the N-(4-dimethylamino 3,5-dinitrophenyl)maleimide have been localized mainly on the oxygen and nitrogen atoms (especially N9, O21, and O22), whereas the regions of nucleophilic reactivity behavior have mainly been delocalized on the carboxylic protons. In this respect, the compound is useful to bond both metallicity and interact intermolecularly.

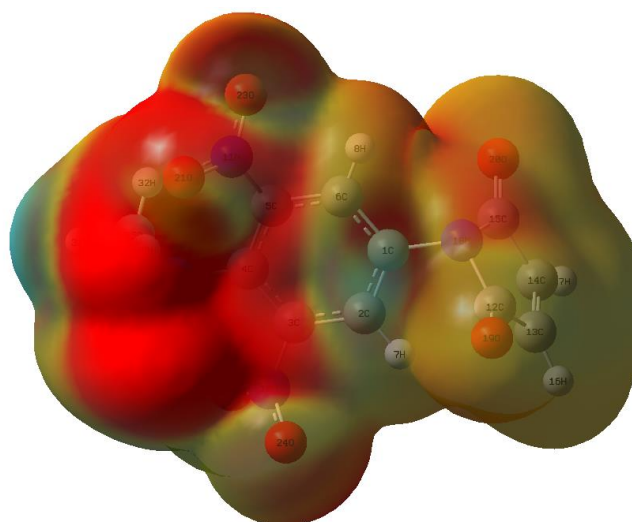


**Figure 5.** 3D plots related to the map of molecular electrostatic potential obtained from DFT method of the N-(4-dimethylamino 3,5-dinitrophenyl)maleimide (red color has displayed the negative regions while blue color has presented the positive regions of MEP). (For interpretation of the references to color in this figure legend, the reader is referred to the web version of the article)

In this part, the electrostatic potential surface (ESP) has been mapped over the electron density that has shown the molecular size, shape, and charge distribution over the N-(4-dimethylamino 3,5-dinitrophenyl)maleimide compound. Moreover, the ESP has enabled us to determine the molecular interaction with one another. We have extensively used the ESP maps to predict reactive behavior, inter and intra-molecular interaction of chemical systems, and hydrogen bonding [58]. On this basis, we have provided the ESP map belonging to the N-(4-dimethylamino 3,5-dinitrophenyl)maleimide in Figure 6 to favor all the findings evaluated from the other parts of the paper. It is obvious from the figure that the most negative regions in the ESP map have been spread over the vicinity of oxygen atoms (electrophilic reactivity regions). Correspondingly, the  $\pi$ -electrons have been noted to delocalize fully over the oxygen atoms. On the other hand, the figure has guaranteed that the carboxyl groups have taken place in the nucleophilic reactivity regions.

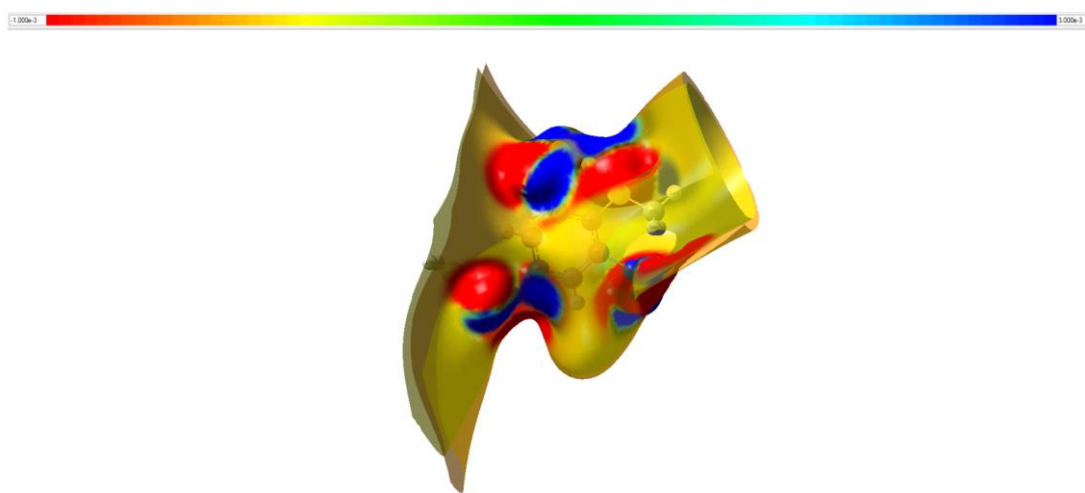


**Figure 6.** 3D plot for an electrostatic potential map of the N-(4-dimethylamino 3,5-dinitrophenyl)maleimide

#### 4. Conclusion

In the current work, we have studied the full characterization of N-(4-dimethylamino 3,5-dinitrophenyl)maleimide molecule with the aid of quantum chemical calculation methods, including the HF/6-311++G(d,p) and DFT-B3LYP/6-311++G(d,p) methods. In this respect, we have determined the optimized molecular structures, vibrational frequencies, thermodynamic features, function groups of structures, nuclear magnetic resonance chemical shifts of C-NMR and H-NMR, charge distributions-dipole moments, molecular charge transfer regions, and spectroscopic characteristic properties for the first time.

Moreover, the observed vibrational frequencies have been compared to the calculated results, and it has been recorded that the experimental data are in good agreement with the computations. The correlation parameters are about  $R^2=0.9996$  and  $R^2=0.9977$  for the vibrational frequencies in the DFT and HF calculation levels, respectively. Thus, we have pointed out the reliability of calculation methods (especially for the DFT-B3LYP/6-311++G(d,p) method).

Besides, we have simulated the electrochemical properties, including the highest/lowest occupied/unoccupied molecular orbital, molecular electrostatic potential, and electrostatic potential maps for the N-(4-dimethylamino 3,5-dinitrophenyl)maleimide compound. The theoretical examinations have shown that the title molecule has exhibited strong non-uniform intra-molecular charge distributions and electron donating groups depending on the actual position of the substituents, electron engagements, lone pairs of electrons,  $\pi$ - $\pi^*$  conjugative effects, and intermolecular hydrogen bonding in the structure. Accordingly, the title compound, including the high electrophilic reactive and nucleophilic regions, can be selected to be a strong terminator for the antimicrobial, anticonvulsant, cytotoxic, antimalarial, and pharmacological microorganisms.

## Author Contributions

All the authors equally contributed to this work. They all read and approved the final version of the paper.

## Conflicts of Interest

All the authors declare no conflict of interest.

## References

- [1] Y. Durust, H. Karakus, M. Kaiser, D. Tasdemir, *Synthesis and anti-protozoal activity of novel dihydropyrrolo [3,4-d] [1,2,3]triazoles*, European Journal of Medicinal Chemistry (48) (2012) 296–304.
- [2] N. Acero, M. F. Brana, L. Anorbe, G. Dominguez, D. Munoz-Mingarro, F. Mitjans, J. Piulat, *Synthesis and biological evaluation of novel indolocarbazoles with antiangiogenic activity*, European Journal of Medicinal Chemistry (48) (2012) 108–113.
- [3] S. N. Lopez, M. Sortino, A. Escalante, F. Campos, R. Correa, V. Cechinel-Filho, R. J. Nunes, S. A. Zacchino, *Antifungal properties of novel N- and alpha, beta-substituted succinimides against dermatophytes*, Arzneimittel-Forschung/Drug Research (53) (2003) 280–288.
- [4] R. Badru, P. Anand, B. Singh, *Synthesis and evaluation of hexahydropyrrolo [3,4-d] isoxazole-4,6-diones as anti-stress agents*, European Journal of Medicinal Chemistry (48) (2012) 81–91.
- [5] A. Ereeg, R. Vukovic, G. Bogdanic, D. Fles, *Free-radical-initiated copolymerization of 2,6-dichlorostyrene with maleimide, n-methylmaleimide and n-phenylmaleimide*, Journal of Macromolecular Science Part A Pure and Applied Chemistry, A37 (5) (2000) 513–524.
- [6] D. Fles, R. Vukovic, *Free-radical-initiated polymerization of 6-maleimidocholesterylhexanoate and 4-maleimidocholesterylbenzoate and copolymerization with  $\alpha$ -methylstyrene*, Journal of Macromolecular Science Part A Pure and Applied Chemistry 32 (8-9) (1995) 1461–1472.
- [7] N. Matuszak, G. Muccioli, G. Laber, D. Lambert, *Synthesis and in vitro evaluation of n-substituted maleimide derivatives as selective monoglyceride lipase inhibitors*, Journal of Medicinal Chemistry 52 (23) (2009) 7410–7420.
- [8] J. R. Cashman, M. MacDonald, S. Ghirmai, K. J. Okolotowicz, E. Serienko, B. Brown, X. Garcio, D. Zhai, R. Dahl, J. C. Reed, *Inhibition of Bfl-1 with n-aryl maleimides*, Bioorganic & Medicinal Chemistry 20 (22) (2010) 6560–6564.
- [9] T. Suzuki, R. Tanaka, S. Hamada, H. Nakagawa, N. Miyata, *Design, synthesis, inhibitory activity, and binding mode study of novel DNA methyltransferase inhibitors*, Bioorganic & Medicinal Chemistry (20) (2010) 1124–1127.
- [10] M. Sortino, F. Garibotto, V. Cechinel Filho, M. Gupta, R. Enriz, S. Zacchino, *Antifungal, cytotoxic and SAR studies of a series of N-alkyl, N-aryl and N-alkyl phenyl-1, 4-pyrrolidones and related compounds*, Bioorganic & Medicinal Chemistry (19) (2011) 2823–2834.
- [11] N. Salewska, J. Boro-Majewka, I. Lacka, K. Chylinska, M. Sabisz, S. Milewski, M. J. Milewska, *Chemical reactivity and antimicrobial activity of N-substituted maleimides*, Journal of Enzyme Inhibition and Medicinal Chemistry 27 (1) (2012) 117–124.

- [12] H. H. Wu, P. P. Chu, *Structure characteristics contributing to flame retardancy in diazo modified novolac resins*, Polymer Degradation and Stability (94) (2009) 987-995.
- [13] T. D. Kim, H. J. Ryu, H. I. Cho, C. H. Yang, J. Kim, *Thermal behavior of proteins: heat-resistant proteins and their heat-induced secondary structural changes*, Biochemistry (39) (2000) 14839-14846.
- [14] J. R. Durig, A. Ganguly, A. M. El Defrawy, G. A. Guirgis, T. K. Gounev, W. A. Herrebout, B. J. Van der veken, *Conformational stability,  $r_0$  structural parameters, barriers to internal rotation and vibrational assignment of cyclobutylamine*, Journal of Molecular Structure 918 (1-3) (2009) 64-76.
- [15] Y. X. Sun, Q. L. Hao, L. D. Lu, X. Wang, X. J. Yang, *Vibrational spectroscopic study of o-, m- and p-hydroxybenzylideneaminoantipyrines*, Spectrochimica Acta Part A: Molecular and Biomolecular Spectroscopy (75) (2010) 203-211.
- [16] Spectral Database for Organic Compounds, [https://sdbs.db.aist.go.jp/sdbs/cgi-bin/direct\\_frame\\_top.cgi](https://sdbs.db.aist.go.jp/sdbs/cgi-bin/direct_frame_top.cgi), Accessed 28.01.2023.
- [17] M. J. Frisch, G. W. Trucks, H. B. Schlegel, G. E. Scuseria, M. A. Robb, J. R. Cheeseman, G. Scalmani, V. Barone, B. Mennucci, G. A. Petersson, H. Nakatsuji, M. Caricato, X. Li, H. P. Hratchian, A. F. Izmaylov, J. Bloino, G. Zheng, J. L. Sonnenberg, M. Hada, M. Ehara, K. Toyota, R. Fukuda, J. Hasegawa, M. Ishida, T. Nakajima, Y. Honda, O. Kitao, H. Nakai, T. Vreven, J. A. Montgomery, Jr., J. E. Peralta, F. Ogliaro, M. Bearpark, J. J. Heyd, E. Brothers, K. N. Kudin, V. N. Staroverov, R. Kobayashi, J. Normand, K. Raghavachari, A. Rendell, J. C. Burant, S. S. Iyengar, J. Tomasi, M. Cossi, N. Rega, J. M. Millam, M. Klene, J. E. Knox, J. B. Cross, V. Bakken, C. Adamo, J. Jaramillo, R. Gomperts, R. E. Stratmann, O. Yazyev, A. J. Austin, R. Cammi, C. Pomelli, J. W. Ochterski, R. L. Martin, K. Morokuma, V. G. Zakrzewski, G. A. Voth, P. Salvador, J. J. Dannenberg, S. Dapprich, A. D. Daniels, O. Farkas, J. B. Foresman, J. V. Ortiz, J. Cioslowski, D. J. Fox, Gaussian, Inc., Wallingford, CT, 2009.
- [18] R. Dennington II, T. Keith, J. Millam, GaussView, Version 4.1.2, Semichem, Inc., Shawnee Mission, KS, 2007.
- [19] A. Saiardi, H. Erdjument-Bromage, A. M. Snowman, P. Tempst, S. H. Snyder, *Synthesis of diphosphoinositol pentakisphosphate by a newly identified family of higher inositol polyphosphate kinases*, Current Biology (9) (1999) 1323-1326.
- [20] S. M. Voglmaier, M. E. Bembenek, A. E. Kaplin, G. Dormán, J. D. Olszewski, G.D. Prestwich, S.H. Snyder, *Purified inositol hexakisphosphate kinase is an ATP synthase: diphosphoinositol pentakisphosphate as a high-energy phosphate donor*, Proceedings of the National Academy of Sciences of the United States of America (93) (1996) 4305-4310.
- [21] A. Saiardi, E. Nagata, H. R. Luo, A. M. Snowman, S. H. Snyder, *Identification and characterization of a novel inositol hexakisphosphate kinase*, Journal of Biological Chemistry (276) (2001) 39179-39185.
- [22] M. J. Schell, A. J. Letcher, C. A. Brearley, J. Biber, H. Murer, R. F. Irvine, *PiUS (Pi uptake stimulator) is an inositol hexakisphosphate kinase*, FEBS Letters (461) (1999) 169-172.
- [23] E. B. Wilson, J. C. Decius, P. C. Cross, Molecular Vibrations: The Theory of Infrared and Raman Vibrational Spectra, Dover Publication Inc., New York, 1980.
- [24] P.W. Atkins, R. S. Friedman, Molecular Quantum Mechanics, 3<sup>rd</sup> edition, Dover Publication Inc., New York, 1996.
- [25] H. Gökçe, S. Bahçeli, *A study of molecular structure and vibrational spectra of copper (ii) halide complex of 2-(2'-thienyl)pyridine*, Journal of Molecular Structure (1005) (2011) 100-106.

- [26] U. Ceylan, G. Ozdemir Tari, H. Gökce, E. Agar, *Spectroscopic (FT-IR and UV-Vis) and theoretical (HF and DFT) investigation of 2-Ethyl-N- [(5-nitrothiophene-2-yl)methylidene] aniline*, Journal of Molecular Structure (1110) (2016) 1-10.
- [27] M. Karabacak, M. Kurt, M. Cinar, A. Coruh, *Experimental (UV, NMR, IR and Raman) and theoretical spectroscopic properties of 2-chloro-6-methylaniline*, Molecular Physics (107) (2009) 253-264.
- [28] N. Sundaraganesan, S. Ilakiamani, H. Saleem, P. M. Wojciechowski, D. Michalska, *FT-Raman and FT-IR spectra, vibrational assignments and density functional studies of 5-bromo-2-nitropyridine*, Spectrochimica Acta Part A: Molecular and Biomolecular Spectroscopy (61) (2004) 2995-3001.
- [29] J. Coates, *Interpretation of Infrared Spectra: A Practical Approach*, John Wiley & Sons Inc., New York, 2000.
- [30] N. P. G. Roeges, *A Guide to Complete Interpretation of Infrared Spectra of Organic Structures*, John Wiley & Sons Inc., New York, 1994.
- [31] T. D. Klots, W. B. Collier, *Heteroatom derivatives of indene Part 3. vibrational spectra of benzoxazole, benzofuran, and indole*, Spectrochimica Acta Part A: Molecular and Biomolecular Spectroscopy (51) (1995) 1291-1316.
- [32] G. Varsányi, *Assignments for vibrational spectra of seven hundred benzene derivatives*, Halsted Press, 1974.
- [33] L. J. Bellamy, *The Infrared Spectra of Complex Molecules*, John Wiley & Sons Inc., New York, 1975.
- [34] R. Silverstein, F. Webster, *Spectroscopic Identification of Organic Compounds*, John Wiley & Sons, New York, 1997.
- [35] Y. Sert, F. Uçun, G. A. El-Hiti, K. Smith, A. S. Hegazy, *Spectroscopic investigations and DFT calculations on 3-(diacetylamino)-2-ethyl-3H-quinazolin-4-one*, Journal of Spectroscopy (7) (2016) 1-15.
- [36] S. Pinchas, D. Samuel, M. Weiss-Brodsky, *The infrared absorption of <sup>18</sup>O-labelled benzamide*, Journal of Chemical Society (1) (1961) 1688-1689.
- [37] M. Tsuboi, *<sup>15</sup>N isotope effects on the vibrational frequencies of aniline and assignments of the frequencies of its nh<sub>2</sub> group*, Spectrochimica Acta (16) (1960) 505-512.
- [38] B. Wojtkowiak, M. Chabanel, *Spectrochimie Moleculaire Technique et Documentation*, Paris, 1977.
- [39] H. Baraistka, A. Labudzinska, J. Terpinski, *Laser Raman Spectroscopy: Analytical Applications*, PWN Polish Scientific Publishers/Ellis Harwood Limited Publishers, 1987.
- [40] L. Rintoul, A. S. Micallef, S. E. Bottle, *The vibrational group frequency of the N-O radical dot stretching band of nitroxide stable free radicals*, Spectrochimica Acta Part A: Molecular and Biomolecular Spectroscopy (70) (2008) 713-717.
- [41] S. Subashchandrabose, H. Saleem, Y. Erdogdu, O. Dereli, V. Thanikachalam, J. Jayabharathi, *Structural, vibrational and hyperpolarizability calculation of (E)-2-(2-hydroxybenzylideneamino)-3-methylbutanoic acid*, Spectrochimica Acta Part A: Molecular and Biomolecular Spectroscopy (86) (2012) 231-241.
- [42] F. Karaboga, U. Soykan, M. Dogruer, B. Ozturk, G. Yildirim, S. Cetin, C. Terzioglu, *Experimental and theoretical approaches for identification of p-benzophenoneoxycarbonylphenyl acrylate*, Spectrochimica Acta Part A: Molecular and Biomolecular Spectroscopy (113) (2013) 80-91.

- [43] N. Tezer, N. Karakus, *Theoretical study on the ground state intramolecular proton transfer (IPT) and solvation effect in two Schiff bases formed by 2-aminopyridine with 2-hydroxy-1-naphthaldehyde and 2-hydroxy salicylaldehyde*, Journal of Molecular Modeling (15) (2009) 223-232.
- [44] J. Z. Zhang, G. Y. Zhao, R. Z. Li, D.Y. Hou, *Time-dependent density functional theory study on the electronic excited state of hydrogen-bonded clusters formed by 2-hydroxybenzonitrile (o-cyanophenol) and carbon monoxide*, Journal of Cluster Science (22) (2011) 501-511.
- [45] D. C. Lee, Y. Jeong, L.V. Brownell, J. E. Velasco, K. A. Robins, Y. Lee, *Theory guided systematic molecular design of benzothiadiazole-phenazine based self-assembling electron-acceptors*, Royal Society of Chemistry Advances (7) (2017) 24105-24112.
- [46] N. Castillo, R. J. Boyd, *A theoretical study of the fluorine valence shell in methyl fluoride*, Chemical Physics Letters (403) (2005) 47-54.
- [47] J. Olsen, P. J. Jørgensen, *Linear and non-linear response functions for an exact state and for an MCSCF state*, The Journal of Chemical Physics (82) (1985) 3235-3264.
- [48] T. U. Helgaker, H. J. A. Jensen, P.J. Jørgensen, *Analytical calculation of MCSCF dipole-moment derivatives*, Chemical Physics (84) (1986) 6280-6287.
- [49] Y. X. Sun, W. X. Wei, Q. L. Hao, L. D. Lu, X. Wang, *Experimental and theoretical studies on 4-(2,4-dichlorobenzylideneamino)antipyrine and 4-(2,6-dichlorobenzylideneamino)antipyrine*, Spectrochimica Acta Part A: Molecular and Biomolecular Spectroscopy 73(4) (2009) 772-781.
- [50] J. B. Foresman, A. Frisch, *Exploring Chemistry with Electronic Structure Methods*, Gaussian Inc., Pittsburgh, PA, 1996.
- [51] G. Gece, *The use of quantum chemical methods in corrosion inhibitor studies*, Corrosion Science (50) (2008) 2981-2992.
- [52] K. Fukui, *Role of frontier orbitals in chemical reactions*, Science (218) (1987) 747-754.
- [53] D. F. V. Lewis, C. Ioannides, D. V. Parke, *Interaction of a series of nitriles with the alcohol-inducible isoform of p450: computer analysis of structure activity relationships*, Xenobiotica (24) (1994) 401-408.
- [54] N. Ozdemir, B. Eren, M. Dincer, Y. Bekdemir, *Experimental and ab initio computational studies on 4-(1hbenzo [d]imidazol-2-yl)-n,n-dimethylaniline*, Molecular Physics (108) (2010) 13-24.
- [55] P. Politzer, J. S. Murray, *The fundamental nature and role of the electrostatic potential in atoms and molecules*, Theoretical Chemistry Accounts (108) (2002) 134-142.
- [56] F. J. Luque, J. M. Lopez, M. Orozco, *Electrostatic interactions of a solute with a continuum. A direct utilization of ab initio molecular potentials for the prevision of solvent effects*, Theoretical Chemistry Accounts (103) (2000) 343-345.
- [57] N. Okulik, A. H. Joubert, *Theoretical analysis of the reactive sites of non-steroidal anti-inflammatory drugs*, Internet Electronic Journal of Molecular Design (4) (2005) 17-30.
- [58] D. L. Wang, X. P. Sun, H. T. Shen, D. Y. Hou, Y. C. Zhai, *A comparative study of the electrostatic potential of fullerene-like structures of Au<sub>32</sub> and Au<sub>42</sub>*, Journal of Chemical Physics Letter (457) (2008) 366-370.